Degradable Self-healable Networks for Use in Biomedical Applications

Mathilde Grosjean, Louis Gangolphe, Benjamin Nottelet

ADVANCED FUNCTIONAL MATERIALS
www.afm-journal.de

Degradable Self-healable Networks for Use in Biomedical Applications

*Mathilde Grosjean, Louis Gangolphe, and Benjamin Nottelet**

Among biomaterials, 3D networks with capacities to absorb and retain large quantities of water (hydrogels) or withstand significant deformation and stress while recovering their initial structures at rest (elastomers) are largely used in biomedical applications. However, when damaged, they cannot recover their initial structures and properties. To overcome this limitation and satisfy the requirements of the biomedical field, self-healable hydrogels and elastomers designed using (bio)degradable or bioeliminable polymer chains have been developed and are becoming increasingly popular. This review presents the latest advances in the field of self-healing degradable/bioeliminable networks designed for use in health applications. The strategies used to develop such networks based on reversible covalent or physical cross-linking or their combination via dual/multi-cross-linking approaches are analyzed in detail. The key parameters of these hydrogels and elastomers, such as mechanical properties, repair and degradation times, and healing efficiencies, are critically considered in terms of their suitabilities in biomedical applications. Finally, their current and prospective uses as biomaterials in the fields of tissue engineering, drug/cell delivery, and medical devices are presented, followed by the remaining challenges faced to ensure the further success of degradable self-healable networks.

1. Introduction

Self-healing polymers were first developed almost fifty years ago.[1] Initially, the main objective was to increase the lifespans of these materials or reprocess them. To this end, scientists began to exploit the interplay between chains to enable repair and restoration of the properties of the original material. The concept was in its infancy, and the starting point for self-repairing polymers was in 2001 when White et al. reported the repair of a fracture in an epoxy resin following the introduction of a repair agent (dicyclopentadiene) and a platinum catalyst.[2] This strategy for incorporating reversible interactions into the polymer chains has since been abandoned. Most strategies to develop self-repairing polymers rely on a single type of reversible covalent bond, sometimes referred to as a dynamic covalent bond (e.g., Diels-Alder (DA) adducts [3] and imine,[4] disulfide,[5] and acylhydrazone bonds [6,7]), or physical noncovalent bond (e.g., hydrogen bonds,[8] hydrophobic, electrostatic,[9] metal-ligand,[10] and host-guest interactions,[11] and π–π stacking [12]). However, a novel generation of dual/multi-cross-linked self-healing materials with several types of chemical and/or physical cross-links has begun to emerge. This is particularly true for degradable polymers that are used in biomedical applications.

Moreover, the use of degradable polymers has been increasing rapidly, scientifically and economically, in the biomedical sector recently, for example, to control the release of drugs or mimic the elastic properties of living tissue.[13–15] In the medical field, they are anticipated to register a compound annual growth rate of 15.7% from 2021 to 2028.[16] Of particular interest are degradable 3D polymer networks with the capacity to absorb and retain large quantities of water (hydrogels) or withstand significant deformation and stress while recovering their initial structures at rest (elastomers).[17–19] The 3D network is formed via physical (hydrogen bonding, dipolar forces, crystalline regions) or chemical (covalent bonding) cross-linking. One advantage of a chemically cross-linked degradable 3D network is its capacity to maintain its 3D structure and lose its mechanical properties homogeneously during degradation (surface erosion). However, when these materials are damaged (cracking, cutting, or scratching), recovering their initial structures and properties is almost impossible.[1] Therefore, introducing self-healing properties into this class of biomaterials is of considerable interest.

Self-healable hydrogels and elastomers have therefore increased in popularity recently, as indicated by the numerous reviews regarding this topic.[1,20–24] However, to date, no review has focused on hydrogels or elastomers with self-healing properties and based on biodegradable or bioeliminable polymer chains, and thus, this review aggregates the latest advances in this field. Readers' attention is drawn to the notion of degradation. Although the networks presented here may be considered degradable, their degradations do not rely on the

M. Grosjean, L. Gangolphe, B. Nottelet
Polymers for Health and Biomaterials
IBMM
Univ Montpellier
CNRS, ENSCM, 34090 Montpellier, France
E-mail: benjamin.nottelet@umontpellier.fr

The ORCID identification number(s) for the author(s) of this article can be found under https://doi.org/10.1002/adfm.202205315.

DOI: 10.1002/adfm.202205315

same mechanism, and thus, two types of degradable networks are considered in this review. First, degradable networks undergoing real degradation, i.e., degradation at the molecular level of the polymer chains (e.g., via hydrolysis in degradable networks or enzymatic reactions in biodegradable networks) that is independent of the reversible/dynamic bonds responsible for the self-healing properties. Second, bioeliminable networks that lose their 3D structures, and whose polymer chains may be excreted by the body without scission of the polymer backbones (e.g., soluble polyethylene glycol (PEG) chains). This review therefore only focuses on networks with (bio)degradable and/or bioeliminable polymers and self-healing properties provided by reversible covalent or dynamic physical cross-linking or dual/multi-cross-linking. In each of these sections, we focus on the mechanical properties, repair and degradation times, and healing efficiencies of the materials, and the last section presents the biomedical applications of these self-healing degradable networks and their prospective uses.

2. Self-Healing Mechanism and Evaluation

Self-healing is based on the presence of reversible bonds and may occur via different mechanisms that may be divided into two main categories: dynamic chemical bonding and reversible physical interactions (**Figure 1**). Reversible covalent bonds include imine, boronate ester, hydrazone, and disulfide bonds and DA adducts. Reversible noncovalent bonding includes hydrogen bonding, hydrophobic, host-guest, electrostatic or ionic interactions, and metal coordination. Self-repairing materials may, therefore, exhibit self-healing properties owing to one or several of these bonds and interactions.

The key process in self-healing is the interpenetration and bond reformation of the polymer chains, with dynamic bonds around the healing interface. Therefore, the incorporation of reversible bonds is not the only prerequisite in preparing a self-healing material, and other factors should be considered. Self-healable materials rely on three principles: 1) localization, 2) temporality, and 3) mobility.[1] First, the concept of localization corresponds to the nature and state (size and position) of the damage, and the latter exhibits an essential effect on the capacity of the material to self-repair (superficial or deep). The repair pathways should be adapted according to the expected damage and application of the material. Second, self-healing is time-dependent, and temporality is defined as the time required for the material to fill the damaged area and regain its initial properties. To accelerate self-healing, the mobility of the chains within the material and the reactivity between the chain ends resulting from the dissociation should be increased, and numerous external factors (pH, temperature, UV light, redox, and mechanical stimuli) are used to realize this.[9,25] The mobility of the polymer chains enables molecular and macroscopic reorganization of the material. At the molecular level, the mobility of the chains enables the dissociation and recombination of cleaved bonds via the diffusion of repairing agents or interplay between the functions involved in the repair process. At the macroscopic level, this mobility results in the visible repair of the damage.[20,26] The necessity of the mobility of the polymer chains and reactivity between the dissociated moieties was clearly established in recent modeling studies, with the polymer chains diffusing across the interface to reform the dynamic bonds, as modeled using diffusion-reaction theory.[27] This theory is based on chain reptation and involves a curvilinear diffusion coefficient combined with the association-dissociation kinetics of dynamic bonds. This enables the prediction of self-healing times and efficiencies as functions of the chain mobility and length distribution, in addition to the bond dynamics (**Figure 2**), and thus, the external stimuli generally used in self-healing.

Notably, the type of damage initially generated varies considerably, rendering the comparison of the self-healing performances of different materials that are also used in a variety of applications challenging.[22] Nevertheless, over the period considered, similar analytical methods were used to evaluate and quantify self-healing macroscopically and at the molecular level. In terms of damage (**Figure 3**), a common method used to macroscopically demonstrate the self-healing capacity of a material is the contact method, which involves cutting the sample into several pieces and placing them in contact to permit self-healing.

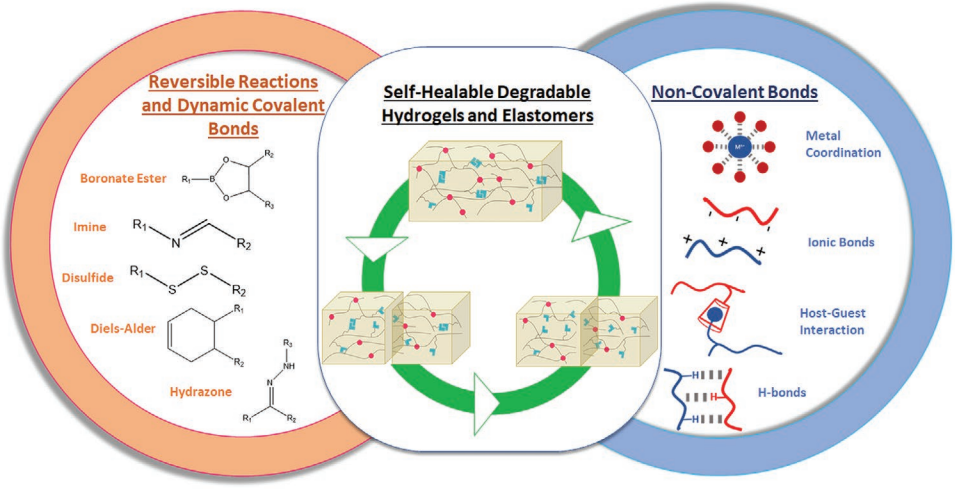

Figure 1. Covalent and non-covalent bonds that allow self-healing properties in hydrogels and elastomers.

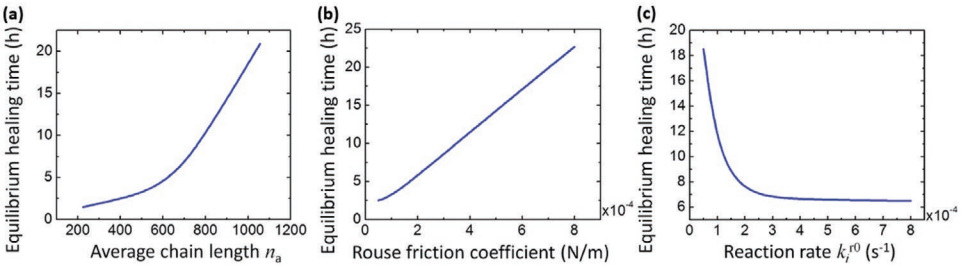

Figure 2. Illustration of the predicted equilibrium healing time based on diffusion-reaction theory in a function of a) the chain length distribution via average chain length b) the chain mobility via the Rouse friction coefficients and c) the bond dynamics via the reverse reaction rates (from dissociated to associated state). Adapted with permission.[27] Copyright 2018, Elsevier.

Punch – a hole is excavated in the material – and crack methods – a crack is generated at the surface of the sample – are two other types of methods reported (Figure 3). Optical evaluation of self-healing includes macroscopic observations, optical microscopy, and scanning electron microscopy (SEM).

At the molecular level, spectroscopic analyses, such as nuclear magnetic resonance spectroscopy, Fourier transform infrared (IR) spectroscopy, and X-ray photoelectron spectroscopy, are historically used to assess dissociation and rebonding. Molecular repair affects the mechanical properties of materials, and self-healing is also assessed by quantifying the mechanical recoveries of materials via static or dynamic mechanical studies. Mechanical evaluations include rheological, tensile, compressive, stretching, bending, and gravity resistance studies. The extent and quality of self-repair are expressed via the self-healing efficiency (SHE), which is obtained by comparing the performance of the healed material with that of the pristine material.

To facilitate a comparison between the networks discussed in this review, readers are invited to refer to the tables in each section, which aggregate the main characteristics listed above (mechanical properties, self-healing evaluation and conditions, SHE, and degradation).

3. (Bio)Degradation versus Bioelimination

This review focuses on hydrogels and elastomers based on (bio)degradable and/or bioeliminable polymers (**Figure 4**). (Bio)degradation refers to the cleavage of the covalent bonds of the polymer backbone (e.g., hydrolysis in degradation and enzymatic lysis in biodegradation), which is accompanied by a decrease in molar mass. Bioelimination refers to the possible excretion of the polymer chains from the body after the loss of the 3D structure of the network but without a decrease in molar mass.

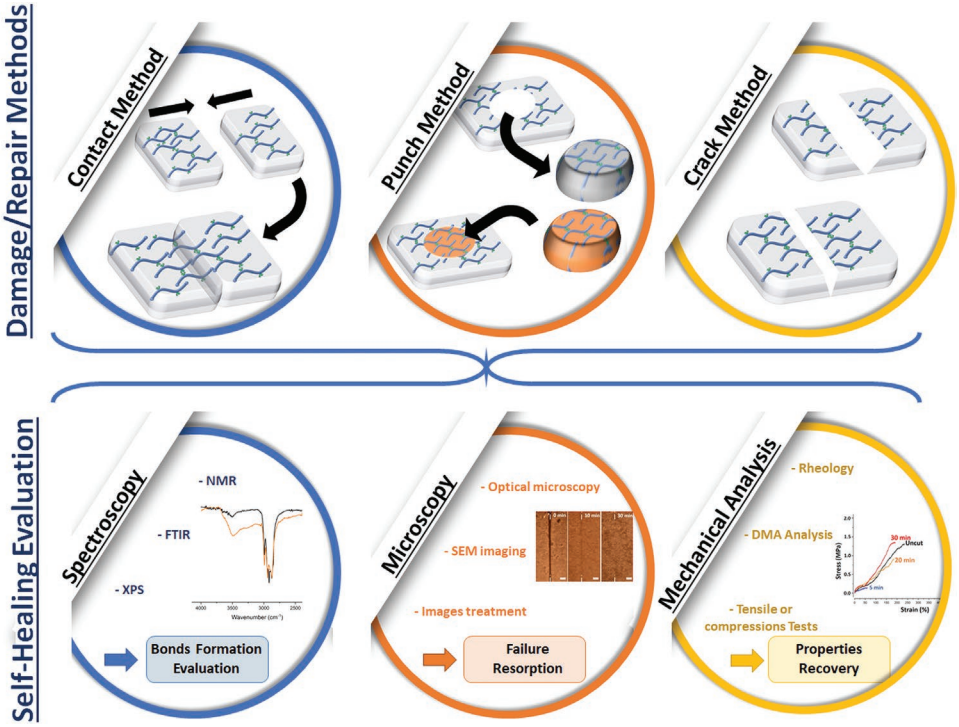

Figure 3. Various methods used to evaluate the self-healing properties.

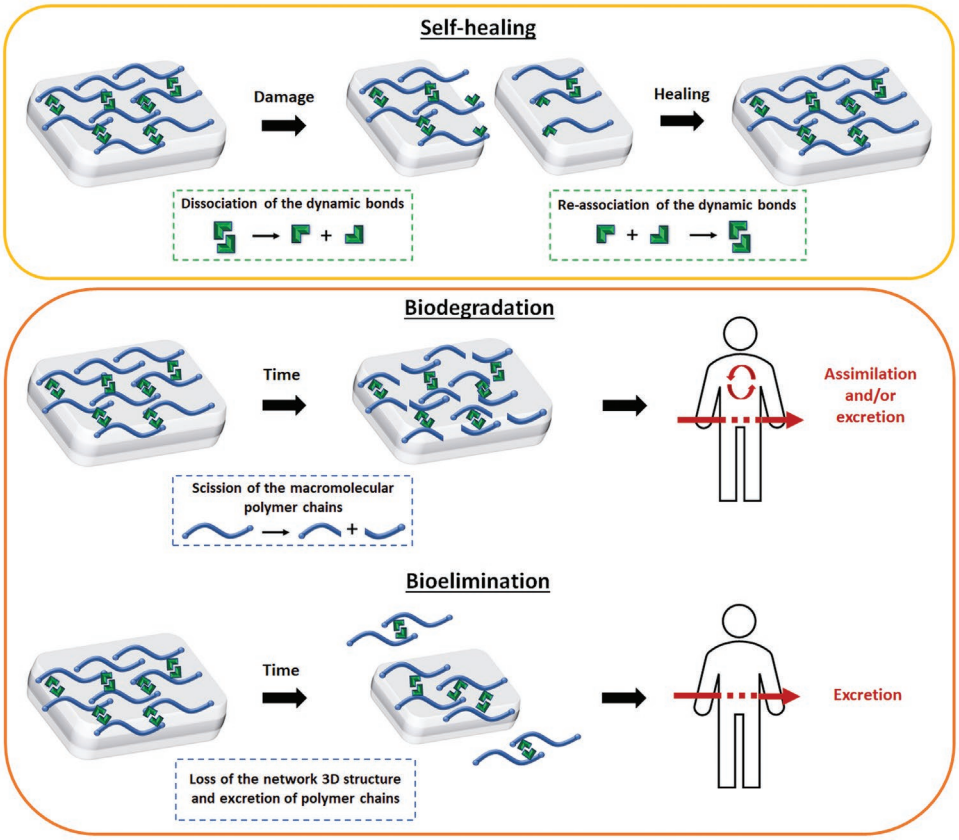

Figure 4. Self-healing versus biodegradation and bioelimination.

Different degradation mechanisms are observed for polymers used in the biomedical field, including hydrolysis, enzymatic degradation, and oxidation.[28] In hydrolysis, the hydrolyzable bonds of polymer chains react with water molecules and dissociate, yielding smaller chains and resulting in polymer degradation. Hydrolytic degradation is thus a combination of water diffusion within the polymer network and random scission of hydrolyzable bonds. Chemical groups that may react with water and undergo hydrolysis mainly contain oxygen, nitrogen, sulfur, and phosphorus atoms. Therefore, polymers that may degrade via this mechanism include polyesters, polyamides, polycarbonates, polyorthesters, and polyanhydrides, and these materials may undergo different degradation processes, such as surface erosion, bulk degradation, and, more rarely, autocatalytic degradation. Surface erosion occurs when hydrolysis is faster than water diffusion. During degradation, the material loses mass progressively but maintains its initial molecular weight and shape. Bulk degradation occurs when water diffusion within the polymer matrix is faster than hydrolysis. The material progressively degrades, eroding from the center to the surface and becoming porous. Oligo- and monomers may diffuse through the material and escape, and thus, the material loses mass. Finally, autocatalytic degradation occurs when bulk degradation leads to the generation of oligomers within the core of the material, which diffuse very slowly but bear functional groups (e.g., carboxylic acid) with the capacity to catalyze hydrolysis. This type of degradation is rare and typical of polylactide species with dimensions of >1 mm.

Degradation via oxidation, which is due to the generation of oxidants by tissues, is caused by the biological defensive action of the immune system. After the implantation of biomedical devices in the body, inflammatory cells may produce oxidative agents (e.g., peroxides) that diffuse into polymeric implants and degrade them. Polymers that are more likely to degrade via oxidation display structures wherein free radicals may be easily generated (e.g., polyethers or polyamines). Degradation via oxidation may also include photodegradation, wherein oxidative agents are generated via exposure to UV or visible radiation.[29]

Enzymatic biodegradation occurs as a defense mechanism in response to the implantation of foreign materials within the body. When acted upon by enzymes, the long polymer chains are reduced to small chains or monomers. Polymer composition is critical in enzymatic degradation, and polymers that may be degraded via this type of reaction include collagens, polysaccharides, proteins, some polyesters, and several polycarbonates. As the enzymes responsible for biodegradation originate from the biological systems of the patients, biodegradation may differ from one individual to another. In the same individual, biodegradation may vary over time and depends on the surrounding tissues. Various enzymes, such as dehydrogenase, oxidase, hydrolase, cutinase, lipase, and protease, play key roles in the biodegradation of polymers.[30]

Notably, these (bio)degradation mechanisms do not rely on reversible or dynamic bonds, which are responsible for the self-healing properties (Figure 4).

4. Degradable Networks With Self-healing Properties Based on Dynamic/Reversible Chemical Bonds

4.1. Imine bond/Schiff base

The imine bonds formed via Schiff-base reactions between amine and aldehyde groups are the most used dynamic covalent bonds in preparing self-healing networks, particularly hydrogels. Examples of self-healing networks based on Schiff-base reactions are shown in **Table 1**, which also shows their mechanical, self-healing, and degradation properties.

Unsurprisingly, among imine bond-containing self-healable degradable hydrogels, most are based on chitosan and its derivatives because of the presence of primary amines within these biopolymers and their good cytocompatibility.[31–38] Conversely, the source of the aldehydes varies, with both synthetic and semi-synthetic biopolymers used. This provides numerous polymer combinations, resulting in chitosan-based self-healable biomaterials with healing times varying from a few minutes to one day and storage modulus G' ranging from a few hundred pascals to a few hundred kilopascals. Although scarcely reported, small aldehydes have also been used, e.g., fluorescent 5-(benzo[d]thiazol-2-yl)-4-hydroxyisophthalaldehyde was associated with chitosan to yield a soft self-healing hydrogel that exhibited a low G' (<100 Pa) and short healing time (<1 h) when exposed to moisture-saturated air.[39]

4.1.1. Schiff-base hydrogels prepared using chitosan and synthetic polymers

Most chitosan/synthetic polymer combinations contain telechelic α,ω-benzaldehyde PEG (PEG-BA). Soft hydrogels with G′ values and self-healing times of 0.5–30 kPa and 1–24 h, respectively, were prepared using various chitosan derivatives. For example, Huang et al. [43] developed hydrogels with G' values of up to 3 kPa, high SHEs (94%), and slow healing rates (12 h at 37 °C) using 4-arm PEG-BA and *N*-carboxymethyl chitosan (CMC). Four-arm PEG-BA was also combined with quaternized methacryloyl chitosan to produce hydrogels that could self-heal within 2 h and exhibited rapid in vivo degradation within 7 d.[44] Depending on the composition of the gel, G' could be tuned between 0.9 and 8 kPa.

Stiffer imine-based hydrogels with high G' values (>10 kPa) were obtained using zwitterionic L-glutamic acid-functionalized chitosan and 4-arm PEG-BA.[45] Following injection through a 22-gauge needle, hydrogels left for 1 h in air and 2 h in phosphate-buffered saline (PBS) exhibited complete self-healed network structures. Increasing the amount of 4-arm PEG-BA cross-linker increased G' from 4 kPa at a chitosan-glutamic acid:PEG-BA ratio of 1:0.33 (w:w) to 31 kPa at a ratio of 1:2. The self-healed samples subjected to mechanical compression displayed mechanical behaviors similar to those of the original hydrogels. The degradation of the hydrogels was investigated at pH values of 6.5 and 7.4. Faster degradation was observed under acidic conditions, with 60% mass remaining after 30 d at pH 7.4 compared to 44% mass remaining after 30 d at pH 6.5.

Other chitosan derivatives associated with PEG-BA include phenol-functionalized chitosan,[40] glycated chitosan with [42] or without [41] fibrin, a chitosan-*g*-aniline tetramer,[33] and *N*-(carboxyethyl)chitosan (CEC).[46] Finally, polyether dibenzaldehyde Pluronic was proposed as an alternative to PEG-BA. In combination with *N*-[3-(4-hydroxyphenyl)propanamido]chitosan, hydrogels with G' values in the range 0.4–1.2 kPa and healing times of 1 h were prepared.[47]

4.1.2. Schiff-base Hydrogels Prepared Using Chitosan and Biopolymers

Self-healable chitosan/biopolymer hydrogels represent the largest class of Schiff-base hydrogels. The biopolymers used include derivatives of hyaluronic acid (HA), dextran, alginate, and cellulose. In contrast to Schiff-base hydrogels based on synthetic polymers, this family of self-healable hydrogels is limited to soft hydrogels with moduli rarely superior to 1 kPa, but with faster self-healing, which is generally observed in <2 h. Hydrogels with healing in minutes (<15 min) were obtained by combining CEC and oxidized sodium alginate (A-Alg) [32] or bisaldehyde-functional carboxymethyl cellulose and CMC.[37] Hydrogels with healing times of <2 h were obtained by mixing glycated chitosan and an oxidized dextran (A-Dex),[35] CMC and A-Dex,[48] or acrylamide-modified chitin with 2% amino groups and A-Alg.[38] Slower self-healing was only reported for injectable electroactive soft degradable hydrogels based on dextran-*g*-aniline tetramer-*g*-4-formylbenzoic acid and CEC, which required 12 h at 37 °C in a humid atmosphere to recover their mechanical properties after damage.[34] With respect to stiffer hydrogels, only three examples with G' values of >1 kPa have been reported recently. These hydrogels were composed of *N*-succinyl-chitosan and multi-aldehyde chondroitin sulfate [31] or CEC and aldehyde-modified HA (A-HA).[36] In the latter example, *N*-(furfural) chitosan was combined with A-Dex in the presence or absence of bismaleimide-PEG to increase the acid resistances of the imine-containing hydrogels by combining the imine bonds with DA adducts.[49]

Regarding biodegradability, all gels exhibited degradation, but with large discrepancies depending on their chemical natures. Whereas several were fully degraded within a few days,[32] others were only partially degraded after a few weeks,[31,35,36] even in the presence of enzymes, such as lysozyme.[37,49]

4.1.3. Schiff-base Hybrid Hydrogels Prepared Using Chitosan and Particles

Using chitosan as a component of the hydrogels, the incorporation of different types of particles also reportedly enhanced the biological and mechanical properties but also slowed the degradation of hydrogels. For example, hydroxyapatite (HAp) nanoparticles and calcium carbonate microparticles were embedded in a self-healing hydrogel composed of CMC and A-Alg.[50]

Table 1. Self-healing hydrogels and elastomers based on imine bonds (materials, mechanical properties, SH evaluation, SH conditions, SHE, and degradation).

Nature	Materials	Mechanical properties	SH evaluation	SH conditions	SHE	Degradation	Ref.
Hydrogel	Phenol-functionalized chitosan/PEG-BA	G' = 0.5 kPa	Cut, Syringe injection	6 h	–	–	[40]
Hydrogel	Glycolated chitosan/PEG-BA	G' = 0.8 kPa at 25 °C G' = 1.5 kPa at 37 °C	Hole	12 h	–	–	[41]
Hydrogel	Glycolated chitosan/PEG-BA	G' = 1.2 kPa	Hole	6h	–	In vitro, 30 d	[42]
Hydrogel	Chitosan-*g*-aniline/PEG-BA	G' = 2 kPa	Cut	Immediately	–	In vivo, 45 d	[33]
Hydrogel	CMC/PEG-BA	G' up to 3 kPa	Cut	12 h, 37 °C	94%	–	[43]
Hydrogel	Quaternized methacryloyl chitosan/PEG-BA	G' = 0.9 to 8 kPa	Cut	120 min, 37 °C	–	In vivo, 7 d	[44]
Hydrogel	Zwitterionic L-GA-chitosan/PEG-BA	G' = 4 to 31 kPa	Syringe injection	1 h in air, 2 h in PBS	–	In vitro, 40% mass loss after 30 d at pH 7.4, 56% at pH 6.5	[45]
Hydrogel	CEC/PEG-BA Polyacrylamide	σ_{max} = 460 kPa ε_{max} = 4600%	Cut	24 h 35 °C, alkaline conditions	84% (σ_{max}) 93% (ε_{max})	–	[46]
Hydrogel	*N*-[3-(4-hydroxyphenyl)propanamido] chitosan/Dibenzaldehyde Pluronic	G' = 0.4 to 1.2 kPa	Syringe injection	1 h	> 95% (G')	–	[47]
Hydrogel	CEC/A-HA	G' = 2 to 6 kPa	Crack	3 min	–	In vitro, 34% mass loss in 10 d	[36]
Hydrogel	N-succinyl-chitosan/Chondroitin sulfate multiple aldehydes	G' = 4 kPa	Cut	2 h, moisture	–	In vivo, 60% degradation in 7w	[31]
Hydrogel	CEC/A-Alg	G' = 0.08 to 2 kPa	Syringe injection	5 min, physiological conditions	–	In vitro, 100% degradation in 3 to 14 d	[32]
Hydrogel	CMC/Aldehyde-functional carboxymethyl cellulose	G' = 200 to 600 Pa	Cut	6 to 15 min	65-83% (G')	In vitro, 50 to 75% mass loss in 3w with lysozyme, 40 to 60% without	[37]
Hydrogel	Glycolated chitosan/A-Dex	G' = 30 Pa to 1 kPa	Syringe injection	120 min	80% (G')	In vitro, 40 to 80% mass loss in 2 weeks	[35]
Hydrogel	CMC/A-Dex	G' = 11 Pa	Cut, Hole	30 min 90 min	–	In vivo, 21 d	[48]
Hydrogel	CEC/Dextran-*g*-aniline tetramer-*g*-4-formylbenzoic acid	G' = 0.3 to 0.65 kPa	Cut	12 h, 37 °C, humid atmosphere	–	In vitro, 74% to 91% degradation in 8 d	[34]
Hydrogel	Acrylamide modified chitin/A-Alg	G' = 600 Pa	Crack	60min	–	–	[38]
Hydrogel	N-furfural chitosan/A-Dex Bismaleimide-PEG	G' = 0.6 to 3 kPa	Cut	3 h 25 °C	100% (G')	In vitro, 20 to 50% degradation with lysozyme	[49]
Hydrogel	CMC/A-Alg HAp $CaCO_3$	G' = 2 to 6 kPa	Syringe injection	–	–	In vitro, 40 to 86% weight loss in 2 weeks	[50]
Hydrogel	CMC/A-Alg MGMs	G' = 3 to 10 kPa	Cut	2 h	97% (G')	In vitro, 10 to 30% mass loss in 2 weeks	[51]
Hydrogel	Chitosan/PEG-BA Fe_3O_4 particles	G' up to 2 kPa	Hole	1 h	–	–	[52]
Hydrogel	CEC/A-HA Carbonyl iron magnetic particles	G' = 1 to 30 Pa	–	–	100% (G')	In vitro, 30 to 75% mass loss in 4d	[53]
Hydrogel	L-arginine conjugated chitosan/PEG-BA pDA-NPs	G' = 230 to 1100 Pa	Cut	5min	–	In vitro, 50 to 75% degradation in 14d	[54]
Hydrogel	CMC/Poly(dextran-*g*-4-formylbenzoic acid) Peptide nanofibers	G' = 91 to 700 Pa	Cut	2min	–	In vitro, 70 to 90% mass loss with lysozyme after 9d	[55]
Hydrogel	Chitosan/Aldehyde functional polyurethane nanoparticles	G' = 700 Pa	Cut	1 h, RT	–	In vitro, 5 to 20% mass loss in 1m	[56]
Hydrogel	Ethylenediamine functional gelatin/Dialdehyde carboxymethylcellulose	G' up to 60 kPa	Cut	1h	90%	In vitro,75% mass loss after 12d, 80% after 2m	[57]

Table 1. Continued.

Nature	Materials	Mechanical properties	SH evaluation	SH conditions	SHE	Degradation	Ref.
Hydrogel	Aldehyde-modified xanthan gum/Phosphatidylethanolamine liposomes	G' = 1 to 100 Pa	Syringe injection Cut	10 min 15min	–	In vitro, in presence of histidine or papain	[58]
Hydrogel	Polyethylenimine/Aldehyde and ammonium functional copolymer poly(4-formylphenyl methacrylate-*co*-2-(methacryloyloxy)ethyl trimethylammonium chloride) PNIPAM	G' = 1 to 2 kPa	Cut	30 min, RT	–	In vitro, 80% mass loss in 24 h at pH 5.4, 37% at pH 7.4	[59]
Elastomer	Synthetic polyester based on terephtaldehyde, tri(2-aminoethyl) amiben trioxatridecanediamine, and dehamethylediamine monomers	E = 1 – 20 MPa σ_{max} = 4.2–16.7 MPa	Crack	3 min, 55 °C	100% (Visual)	In vitro, 100% degradation after 48 h at pH = 1	[60]

A-Alg, aldehyde-modified alginate; A-Dex, aldehyde-modified dextran; A-HA, aldehyde-modified hyaluronic acid; CEC, carboxyethyl chitosan; CMC, carboxymethyl chitosan; E, Young's modulus; G', storage modulus; HAp, hydroxyapatite; L-GA, L-glutamic acid; MGMs, magnetic gelatin microspheres; PDA-NPs, polydopamine nanoparticles; PEG, poly(ethylene glycol); PEG-BA, benzaldehyde poly(ethylene) glycol; PNIPAM, poly(N-isopropylacrylamide); ε_{max}, strain at break; σ_{max}, stress at break.

This led to an increase in G' to 6 kPa compared with that of 2 kPa without particles. It also stabilized the network, which displayed a limited mass loss of 40% compared to that of 86% without particles after 2 weeks. Various magnetic particles have been incorporated to produce hydrogels with magnetic field-dependent rheological properties. To this end, magnetic gelatin microspheres (MGMs) loaded with Fe_3O_4 nanoparticles were added to a CMC/A-Alg hydrogel,[51] Fe_3O_4 particles were mixed into a chitosan/PEG-BA matrix,[52] and carbonyl iron magnetic particles were added to CEC/A-HA.[53]

To improve the mechanical properties and increase the stabilities of hydrogels, Ling et al. [54] prepared hydrogels with L-arginine-conjugated chitosan and PEG-BA containing polydopamine nanoparticles (pDA-NPs) that enabled an increase in G' of ≈400%. Conversely, an increase of 66% was reported by Qiu et al. [55] upon reinforcement of CMC/poly(dextran-*g*-4-formylbenzoic acid) hydrogels with peptide nanofibers. Finally, a hybrid system composed of chitosan and aldehyde-functional polyurethane (PU) nanoparticles yielded Schiff-base self-healing hydrogels.[56] PU was obtained via the reaction of polycaprolactone (PCL) diol and poly(1,4-butylene adipate) (HTPBA) diol with isophorone diisocyanate (IPDI) and modified with glyoxal. After damage, the gel fully healed after 1 h at room temperature and could endure stretching without breaking, whereas, under repeated damage-healing cycles under oscillatory strain, it fully recovered its initial G' at ≈ 700 Pa. The latter example displayed the slowest in vitro degradation, with a limited mass loss of 20% after one month.

4.1.4. Other Schiff-base hydrogels

Other examples of self-healable hydrogels based on Schiff bases but without chitosan as the source of primary amine groups have been reported. Lei et al. [57] prepared a stiff self-repairing hydrogel using ethylenediamine-functionalized gelatin that reacted with dialdehyde carboxymethyl cellulose. Such hydrogels exhibited high G' values compared to those of the other systems, with G′ values of up to 60 kPa, high SHEs of 90% after 1 h, and rapid initial degradation, with 25% mass remaining at day 12. Ma et al. [58] developed a biodegradable, injectable polymer-liposome hydrogel based on aldehyde-modified xanthan gum cross-linked with phosphatidylethanolamine liposomes. The hydrogel exhibited rapid self-healing (<15 min) but a low G' of 1–100 Pa. Remarkably, degradation depended on the environment. It was rapid in the presence of histidine, due to substitution within the original Schiff-base linkages, or papain, due to xanthan enzymatic degradation, but no degradation was observed in water.

Finally, using fully synthetic, potentially eliminable polymers, Wang et al. [59] reported an injectable Schiff base-containing hydrogel with thermoresponsive and antimicrobial properties obtained by combining aldehyde- and ammonium-functionalized poly(4-formylphenyl methacrylate-*co*-2-(methacryloyloxy) ethyl trimethylammonium chloride), poly(*N*-isopropylacrylamide) (PNIPAM), and polyethylenimine.

4.1.5. Schiff-base elastomers

As demonstrated by these examples, Schiff-base dynamic cross-linking is a powerful, widely used approach in designing degradable, self-healing hydrogels. However, this strategy remains in its infancy in yielding degradable, self-healing elastomers for use in biomedical applications, with only one example reported to date. Li et al. designed dynamic covalent elastomers using terephthaldehyde, various diamines, and tri(2-aminoethyl)amine as cross-linking agents.[60] The networks obtained displayed glass transition temperatures (T_g) of 7–60 °C, strain at break (ε_{max}) values of up to 170%, and stress at break (σ_{max}) values of 1–20 MPa. However, they exhibited mostly plastic behaviors rather than elastomeric behaviors, with marked plastic deformations. Self-healing was realized upon heating to enable chain motion, which was applied to the scratched samples, with healing temperatures ranging from 20 to 55 °C. Although not composed of degradable precursors, this material could fully disintegrate within 48 h under acidic conditions.

Table 2. Self-healing hydrogels based on boronate ester bonds (materials, mechanical properties, SH evaluation, SH conditions, SHE, and degradation).

Nature	Materials Boronic polymer/Diol polymer	Mechanical properties	SH evaluation	SH conditions	SHE	Degradation	Ref.
Hydrogel	Poly(methacryloyloxyethyl phosphorylcholine) functionalized with benzoxaborole or catechol pendant groups	G' = 0.1 kPa	Cut	1 min	–	In vitro, 20 min in the presence of fructose, immediately with HCl 0.1 M	[61]
Hydrogel	5-methacrylamido-1,2-benzoxaborole 3-gluconamidopropyl methacrylamide Acrylamide	G' = 1 kPa	Cut	5 min	–	–	[62]
Hydrogel	MAABO/Nopoldiol 2-glucoamidoethylmethacrylamide PEG methyl ether methacrylate	G' = 10 Pa to 4 kPa	Cut	20 s	–	In vitro, in the presence of H_2O_2	[63]
Hydrogel	Poly(DMA-st-MAABO) 2-lactobionamidoethyl methacrylamide, exhibiting galactose residues on the surface		Cut	1 min	–	In vitro, in the presence of fructose, ATP, H_2O_2, or in acidic conditions	[64]
Hydrogel	Phenylboronic acid modified 4-armed PEG/ Dopamine functionalized 4-armed PEG	G' = 20 kPa	Cut	30 s	–	In vitro, acidic or basic conditions, in the presence of glucose or dopamine	[65]
Hydrogel	Poly(aspartic acid) derivatives with boronic acid groups/PVA	G' = 200 to 400 Pa	Cut	1 min, 1 h, or 12 h depending on the composition	100% (G')	–	[66]
Hydrogel	Alginate grafted with phenylboronic acid/PVA	G' = 1 kPa	Cut	30 s	100% (G')	–	[67]
Hydrogel	Carboxyethyl cellulose grafted with phenylboronic acid/PVA	G' = 40 to 1000 Pa	Cut	12 h	>95% (σ_{max}) 100% (G')	–	[68]
Hydrogel	3-aminophenylboronic acid modified sodium alginate/Methacrylated hyaluronic acid	G' = 300 Pa	Cut, Hole	10 min	100% (G')	In vivo	[69]
Hydrogel	Poly(acrylamide-*co*-dopamine methacrylamide) bis(phenylboronic acid carbamoyl) cystamine/PVA	G' = 1 kPa	Cut	1 to 5 min	100% (G')	–	[70]
Hydrogel	CTL Boric acid Mannitol	G' = 20 Pa	Cut	5 min	–	In vitro, in the presence of lysozyme	[71]

CTL, lactose modified chitosan; DMA, *N*-*N*-dimethylacrylamide; G', storage modulus; MAABO, 5-methacrylamido-1,2-benzoxaborole; nopoldiol, (1R)-(-)-nopol-methacrylamido-diol; PVA, poly(vinyl alcohol); σ_{max}, stress at break.

4.2. Boronate Ester Bond

The use of reversible boronate ester bonds is another method of preparing self-healing degradable hydrogels, as indicated by the larger number of biomaterials developed recently containing these bonds (**Table 2**). Boronate ester bonds are formed via the complexation of boronic acid and diol, and their stabilities depend on the pH and concentration of free alcohol groups acting as binding competitors (e.g., glucose in vivo). If the pH is higher than the pKa of the diol (generally below alkaline pH), the ionization of the diol may be initiated, leading to the formation of a stable borate ester. Numerous boronic acid derivatives have been developed, but oxa- and benzoxaboroles are the most common, whereas sugar derivatives or catechol groups are classically used as diols/polyols.

Two strategies yield boronate ester-based self-healable materials, depending on the natures of the partners bearing the complementary reactive groups, which may be two polymers (synthetic or biopolymers) or a polymer and low-molecular-weight compound. These distinctions are used to classify the various examples. Notably, owing to the reversibility of the boronate ester bond under various conditions (competitors, pH, oxidation), it is a bond of choice in designing networks using non-degradable polymers while guaranteeing their bioelimination.

4.2.1. Boronate Ester-based Hydrogels Prepared Using Synthetic Polymers

Among the synthetic polymers, polyacrylic derivatives bearing (benz)oxaborole groups have mainly been used to yield boronate ester-based hydrogels. Such hydrogels are soft and typically exhibit rapid self-healing times of <5 min, e.g., very soft catechol-based hydrogels (G' = 0.1 kPa) were designed using zwitterionic copolymers of poly(methacryloyloxyethyl phosphorylcholine) functionalized with benzoxaborole or catechol pendant groups.[61]

Among the acrylic monomers containing oxaborole groups used to yield self-healable hydrogels, 5-methacrylamido-1,2-benzoxaborole (MAABO) is commonly used. MAABO was copolymerized with 3-gluconamidopropyl methacrylamide and acrylamide.[62] Poly(ethylene glycol) methyl ether methacrylate was also copolymerized with MAABO, (*1R*)-(–)-nopol-methacrylamido-diol and 2-gluconamidoethyl methacrylamide to prepare dual-cross-linked hydrogels that exhibited self-healing properties in a wide range of pH values (8.5–1.5) and degradabilities under oxidative conditions.[63] Finally, cross-linked nanogels of NIPAM, *N,N*-methylenebisacrylamide, and 2-lactobionamidoethyl methacrylamide, bearing galactose residues on their surfaces, were used as cross-linkers to form a hydrogel network via the formation of dynamic adducts with the benzoxaborole groups of hydrophilic poly(dimethylacrylamide (DMA)-*co*-MAABO) copolymers.[64]

In addition to polyacrylics, a few examples of fully synthetic boronate ester-based hydrogels, which were prepared using PEG or polyvinyl alcohol (PVA), have been reported. Injectable hydrogels based on dopamine-functionalized 4-arm PEG and phenylboronic acid-modified 4-arm PEG exhibited *G′* values of 20 kPa and short self-healing times of 30 s.[65] In another example, PVA was mixed with poly(aspartic acid) derivatives bearing quaternary ammonium groups with bactericidal properties and boronic acid groups to yield materials with G′ values of 200–400 Pa with fast (1 min) or slow (up to 12 h) healing times.[66]

In addition to their rapid self-healing properties, these boronate ester-based hydrogels displayed good cytocompatibility and could be easily degraded under competitive exchange (e.g., with fructose, adenosine triphosphate, or dopamine), oxidative (e.g., with hydrogen peroxide), or acidic conditions.

4.2.2. Boronate Ester-based Hydrogels Prepared Using Biopolymers

Biopolymers have been used to develop boronate ester-based hydrogels by exploiting the ease of functionalization provided by the reactive groups on their backbones. PVA was combined with alginate grafted with phenylboronic acid to yield a hydrogel that healed in only 30 s,[67] whereas its association with carboxyethyl cellulose grafted with phenylboronic acid led to gels requiring 12 h to heal.[68] In another example, methacrylated HA was associated with 3-aminophenylboronic acid-modified sodium alginate to develop soft hydrogels (*G′* = 300 Pa) with short self-healing times of 10 min.[69]

4.2.3. Boronate ester-Based Hydrogels Formed via the Associations of Polymers and Low Molecular Weight Cross-linkers

Low-molecular-weight polyboronic or polyol compounds have been used as cross-linkers to yield boronate ester-based hydrogels. Using a bis(phenylboronic acid carbamoyl) cystamine cross-linker with PVA and poly(acrylamide-*co*-dopamine methacrylamide), Guo et al. prepared soft gels, which displayed *G′* values of 1 kPa and rapid self-repair times of <5 min.[70] Boric acid and lactose-modified chitosan (CTL) were combined in the presence of the polyol competitor mannitol to reduce the very fast kinetics of CTL/boron self-assembly and avoid syneresis to form homogeneous but weak gels (*G′* ≈ 20 Pa) under physiological conditions.[71] These CTL-boric acid gels were repaired after 5 min and stretched by >500%.

4.3. Hydrazone Bond

Hydrazone bonds are reversible covalent bonds formed via reactions between aldehyde and hydrazine groups. Owing to their sensitivities to pH, they are the cornerstones of numerous biodegradable self-healing hydrogels. Similar to imine bond-based materials, most systems described include at least one biopolymer in their design, whereas only a few examples of fully synthetic materials are reported in the recent literature (**Table 3**).

4.3.1. Hydrazone-based Hydrogels Prepared Using Biopolymers

Qin et al. contributed to the development of such hydrazone-based hydrogels with a light-emitting self-healable hydrogel prepared using tetraphenylethylene-poly(*N,N*-dimethylacrylamide-stat-diacetone acrylamide)$_2$ and acylhydrazide-functionalized pectin [72] and a hydrogel composed of pectin aldehyde and acylhydrazide-functionalized poly(NIPAM-stat-acylhydrazide).[73] Both hydrogels could heal in 24 h, degraded upon exposure to a pectinase solution, and exhibited G′ values of ≈ 1 kPa, regardless of the concentrations or ratios investigated. Stiffer hydrogels with G′ values of >3 kPa were obtained by mixing aldehyde- and hydrazide-functionalized HAs.[74] Softer hydrogels (*G′* < 1 kPa) were prepared by mixing adipic dihydrazide-grafted carboxyethyl chitin and PEG-BA,[75] cross-linking oxidized xanthan with an 8-arm PEG-hydrazine,[76] or mixing hyperbranched PEG-based multi-hydrazide, A-HA, and gelatin.[77] These soft gels healed within 2–24 h and displayed slow mass losses when incubated in buffer solutions. For instance, a maximum degree of degradation of 9.2% after 30 d at pH 7.4 and 36.8% at pH 5.5 were obtained for the xanthan-PEG system. However, degradation could be significantly increased in the presence of collagenase [74] or lysozyme.[75]

Finally, two self-healing hydrogels that exhibited degradabilities under specific conditions were reported. Chen et al. fabricated hydrogels using pectin acylhydrazide and poly(DMA-*stat*-4-formylphenyl acrylate (FPA)).[78] When exposed to sodium carbonate, the gels degraded in 24 h, whereas degradation required ≈ 1 week with sodium bicarbonate. In another example, hydrogels prepared using A-HA and 3,3′-dithiobis(propionic hydrazide) were developed to provide a variety of degradation kinetics ranging from 4 h to 5 weeks, depending on the redox and enzymatic conditions.[79] Both gels exhibited G′ values of ≈ 2 kPa and self-healed within a few hours.

4.3.2. Hydrazone-based Hydrogels Prepared Using Synthetic Polymers

Qin et al. developed fully synthetic hydrazone-based self-healing hydrogels with G′ values of ≈ 1 kPa. Acylhydrazone-containing hydrogels were prepared by cross-linking P(NIPAM-FPA-DMA) copolymers with 3,3′-dithiobis(propionohydrazide) or

Table 3. Self-healing hydrogels based on hydrazone bonds (materials, mechanical properties, SH evaluation, SH conditions, SHE, and degradation).

Nature	Materials Aldehyde polymer/Hydrazine polymer	Mechanical properties	SH evaluation	SH conditions	SHE	Degradation	Ref.
Hydrogel	Tetraphenylethylene-poly(DMA-*stat*-diacetone acrylamide)$_2$/Acylhydrazide functionalized pectin	G' = 0.6 to 2 kPa	Cut	24 h, moisture	–	–	[72]
Hydrogel	Pectin aldehyde/ Poly(NIPAM-*stat*-acylhydrazide)	G' = 1 kPa	Cut	24 h	–	In vitro, in the presence of pectinase or by microbes from the air	[73]
Hydrogel	A-HA/Hydrazide-HA	G' > 3kPa	–	–	100% (G')	In vitro, increased in the presence of collagenase	[74]
Hydrogel	PEG-BA/Adipic dihydrazide-grafted carboxyethyl chitin Phe-NH_2	G' = 1 to 13 Pa	Cut	6 h, 37 °C, humid environment	95% (compressive load)	In vitro, increased in the presence of lysozyme	[75]
Hydrogel	Oxidized xanthan/8-arm PEG-hydrazine	G' = 190 to 770 Pa	Cut	24 h, 37 °C		In vitro, 9% degradation after 30 d at pH 7.4, 37% at pH 5.5	[76]
Hydrogel	A-HA/Multi-hydrazide PEG Gelatin	G' = 200 to 400 Pa	Cut	2h	–	–	[77]
Hydrogel	Poly(DMA-*stat*-4-FPA)/Pectin achlydrazide	G' = 2 kPa	Cut	12 h, moisture	–	In vitro, 24 h in Na_2CO_3, 1 week in $NaHCO_3$	[78]
Hydrogel	A-HA/3,3′-dithiobis(propionic hydrazide)	G' = 2.2 kPa	Cut	2 h	100% (G')	In vitro, 5 weeks in PBS, 4 h in dithiothreitol, 12 to 17 h in H_2O_2, 12 to 16 h in hyaluronidase, or under UV-light	[79]
Hydrogel	P(NIPAM-FPA-DMA)/3,3′-dithiobis (propionohydrazide), PEO dihydrazide	G' = 30 Pa to 5kPa	Hole	24 h	–	In vitro, 24 h in Na2CO3 and TEA	[6]
Hydrogel	Dialdehyde-PEG/PAEH	G' = 1 kPa	Cut	24 h	–	In vitro, 7d in Na_2CO_3, 1m in $NaHCO_3$	[80]

A-HA, aldehyde-modified hyaluronic acid; DMA, *N*-*N*-dimethylacrylamide; FPA, formylphenyl acrylate; G', storage modulus; HA, hyaluronic acid; NIPAM, N-isopropylacrylamide; PAEH, poly(aspartic acid) derivatives with hydrazide functional groups; PEG, poly(ethylene glycol); PEG-BA, benzaldehyde poly(ethylene glycol); PEO, poly (ethylene oxide).

PEG-dihydrazide of various molecular weights.[6] They also prepared hydrogels using hydrazide-functionalized poly(aspartic acid), which was reacted with PEG-dialdehyde.[80] All hydrogels self-healed in 24 h and degraded in sodium carbonate solutions after 24 h (the former) or 7 d (the latter).

4.4. Disulfide Bond

Disulfide bonds are among the most commonly used reversible covalent bonds because of their natural occurrence in proteins, and they are critical in protein bioactivities. Disulfide bonds are the oxidized partners of the thiol/disulfide redox couple, and thus, they are easily converted to their thiol counterparts upon reaction with thiols at neutral pH or nucleophilic thiolates at alkaline pH. In contrast to the previously discussed dynamic chemical bonds, disulfide bonds are rarely used in designing degradable self-healing hydrogels. Only one example has been reported in the recent literature, whereas several self-healable disulfide-based elastomers have been reported (**Table 4**).

4.4.1. Disulfide Bond-based Hydrogels

Zhang et al. [81] developed an inherently biodegradable self-healing hydrogel based on bovine serum albumin (BSA), wherein the network structure could reversibly form via the reduction of the disulfide bonds in BSA, followed by re-oxidation. The gels were soft, with G′ values of 1 kPa, could fully self-heal in 2 min in the presence of hydrogen peroxide, and were biocompatible, as demonstrated using MCF-7 cells.

4.4.2. Disulfide Bond-based Elastomers

Although disulfide bonds are not commonly reported in self-healable hydrogels, they have been investigated for their self-healing properties in elastomers. This approach is a component of the general trend aimed at reducing chemical and plastic waste, as these self-healable elastomers are considered sustainable because of their reprocessabilities. Soft elastomers were prepared using a bis(acrylate) monomer (bis(2-(acryloyloxy) ethyl)octadic-9-enedioate) mixed with copolymers of polydimethylsiloxane containing 4–6% (mercaptopropyl)methylsiloxane to formulate an ink for use in 3D printing technology.[82] Thin films with thicknesses of 1 mm exhibited respective E, σ_{max}, and ε_{max} values of 0.2 MPa, 52 kPa, and 24% at room temperature. Self-healing was realized via heating at 80 °C for 8 h, which led to SHEs of 86% and 100% in terms of tensile strain and strength, respectively. In another example, Yuan et al. prepared self-healing elastomers via the polycondensation of dicarboxylic acids, 1,4-butanediol, glycerol, and 3,3′-dithiodipropionic acid (DTPA).[83] Glycerol and DTPA were used to modulate the properties of the soft elastomers, with E, σ_{max}, and ε_{max} values in the ranges 0.2–0.9 and 0.4–1.5 MPa and 550–1700%, respectively, as functions of the compositions. Self-healing at 30 °C

Table 4. Self-healing hydrogels and elastomers based on disulfide bonds or Diels-Alder adducts (materials, mechanical properties, SH evaluation, SH conditions, SHE, and degradation).

Nature	Mechanism	Materials	Mechanical properties	SH evaluation	SH conditions	SHE	Degradation	Ref.
Hydrogel	Disulfide bonds	BSA	$G' = 1$ kPa	Cut	2 min, H_2O_2	100% (σ_{max})	–	[81]
Elastomer	Disulfide bonds	Polyester based on bis(acrylate) monomer (bis(2—(acryloyloxy)ethyl) octadic-9-enedioate) with [4–6% (Mercaptopropyl)-methylsiloxane]-dimethyl siloxane	$E = 0.23$ MPa $\sigma_{max} = 52$ kPa $\varepsilon_{max} = 24\%$	Cut	8 h, 80 °C	86% (ε_{max}) 100% (σ_{max})	–	[82]
Elastomer	Disulfide bonds	Polyester via polycondensation of dicarboxylic acids, 1,4-butanediol, glycerol, and DTPA	$E = 0.16$–0.86 MPa $\sigma_{max} = 0.36$–2.42 MPa $\varepsilon_{max} = 542$–1728%	Cut	2 h, 30 °C	100% (scratch) 95–98% ($\sigma_{max}/\varepsilon_{max}$)	–	[83]
Elastomer	Disulfide bonds	Polyurethane block copolymers: hydroxy-terminated poly(1,4-butylene adipate) (HTPBA), IPDI, and PCL diol as a soft segment	$E = 7.2$ MPa $\sigma_{max} = 4.6$ MPa	Cut	5 h, RT 2 h, 40 °C	95% (σ_{max})	In vitro, 50% mass loss (8d, pH 14)	[84]
Elastomer	Diels-Alder	PCL-furan/PCL-maleimide	$E = 75 - 159$ MPa $\varepsilon_{max} = 202$–536%	Cut	1 h, 100 °C then 24 h, 50 °C	100% (Visual) 60–100% (E)	–	[90]
Elastomer	Diels-Alder	PCL-furan/PCL-maleimide	$E = 19.6$–347.9 MPa $\sigma_{max} = 0.79$–27.1 MPa $\varepsilon_{max} = 17$–36%	Scratch	24 h, 60 °C	91–100% (E)	–	[89]

BSA, bovine serum albumin; DTPA, dithiopropionic acid; E, Young's modulus; G', storage modulus; HTPBA, hydroxy-terminated poly(1,4-butylene adipate); IPDI, isophorone diisocyanate; PCL, polycaprolactone; ε_{max}, strain at break; σ_{max}, strain at break.

was realized visually after 1 h, whereas σ_{max} recovery required 2 h (**Figure 5**.1). Using a similar polycondensation strategy in the design of a conductive skin device, Li et al. synthesized PUs with disulfide bonds in their backbones using hydroxy-terminated HTPBA, IPDI, and PCL diol.[84] Optimization of the composition enabled E and σ_{max} to reach 7.2 and 4.6 MPa, respectively, while self-healing was realized after 2 h at 40 °C with a SHE in terms of tensile strength of 95%.

4.5. DA Adducts

DA cycloaddition reactions have been investigated to extend the service lifetimes of materials. This is a reversible reaction between furan and maleimide groups under a thermal stimulus. Despite the covalent nature of DA chemistry, its bond strength is lower than those of other covalent bonds. Therefore, upon crack initiation, the DA adducts could cleave via

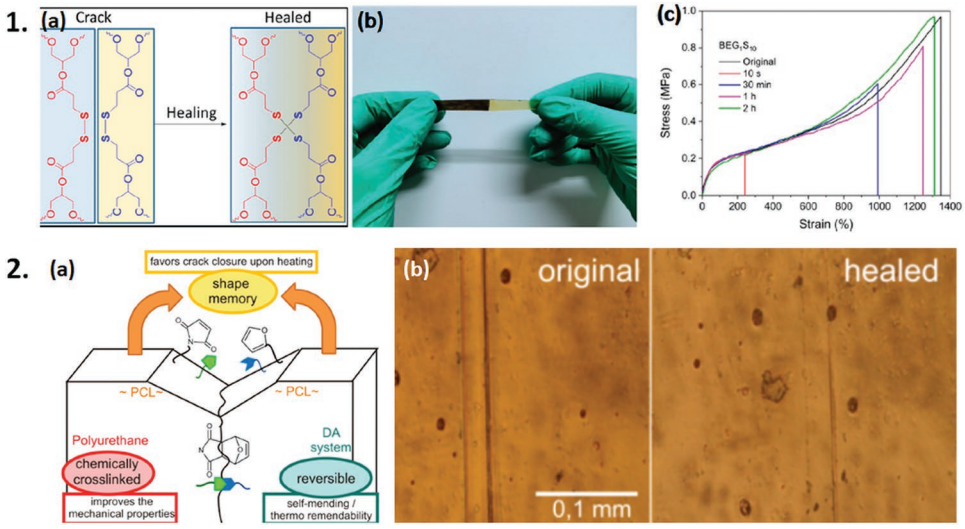

Figure 5. 1) a) Theoretical mechanism for self-healing of a disulfide-based elastomer b) Image showing self-healing of recombined cut elastomers after being kept at room temperature (30 °C) for 10 s, c) stress-strain curves of the original and healed elastomers with different healing times at room temperature. 2) a) Schematic depiction of the Diels-alder-based shape memory-assisted self-healing process in a polyurethane material based on furan-maleimide chemistry b) Optimal microscopy of sample cut with a razor blade before (left) and after (right) healing at 50 °C for 24 h. Adapted with permission.[83,90] Copyright 2020, American Chemical Society. Copyright 2014, American Chemical Society.

Table 5. Self-healing hydrogels and elastomers based on hydrogen bonds (materials, mechanical properties, SH evaluation, SH conditions, SHE, and degradation).

Nature	Materials	Mechanical properties	SH evaluation	SH conditions	SHE	Degradation	Ref.
Hydrogel	Cytosine and guanosine-modified HA 1,6-hexamethylenediamine	G' = 0.85 to 99.80 kPa	Cut	24h	–	In vitro, 40% mass loss in 7 d	[91]
Hydrogel	BSA Epychlorhydrin	G' = 10 to 10 000 Pa	Cut	24h	–	In vitro, 70% degradation in 72 h with trypsin, only 12% in PBS	[92]
Elastomer	PLA-PEB-UPy	E = 4.4 to 156 MPa σ_{max} = 2.2 to 9.4 MPa ε_{max} = 125 to 691%	Cut	20 min, UV-light, 76 °C	97% (E)	–	[93]
Elastomer	PDLLA-UPy	E = 594 to 900 MPa σ_{max} = 8.0 to 9.6 MPa	Cut	270 s, 37 °C	100% (Visual)	–	[94]
Elastomer	PLA-*co*-PTHF with UPy	E = 56.9 MPa σ_{max} = 1.1 to 14.8 MPa	Cut Crack	24 h, 80 °C	99% (σ_{max})	–	[95]
Elastomer	UPy to telechelic PTMEG 4-arm star-shaped PCL	E = 44 to 117 MPa σ_{max} = 3.24 to 8.25 MPa ε_{max} = 18 to 54%	Cut	48 h, 40 °C	88% (σ_{max})	–	[96]
Elastomer	Dimethacrylate PCL Methacrylates bearing UPy function	E = 170 to 203 MPa σ_{max} = 10 to 14 MPa ε_{max} = 200 to 450%	Deep scratch	1 h, 80 °C	80% (σ_{max})	–	[97]
Elastomer	PGS with UPy	E = 0.4 to 32.8 MPa σ_{max} = 0.2 to 4.6 MPa ε_{max} = 63 to 260%	Cut	12 h, 55 °C	85% (σ_{max})	In vitro, 88% mass loss with enzyme after 84h	[98]
Elastomer	PSeD with UPy	E = 1.9 to 10.6 MPa σ_{max} = 1.9 to 2.7 MPa ε_{max} = 121 to 215%	Cut	30 min, 60 °C	98% (σ_{max})	In vitro, 79% mass loss with enzyme after 48h	[99]

BSA, bovine serum albumin; E, Young's modulus; G', storage modulus; HA, hyaluronic acid; PCL, polycaprolactone; PDLLA, poly(D,L-lactic acid); PGS, poly(glycerol-*co*-sebacate); PLA, poly(lactic acid); PSeD, poly(sebacoyl diglyceride); PTHF (poly(tetrahydrofuran); PTMEG, poly(tetramethylene ether) glycol; UPy, 2-ureido-4[1H]-pyrimidinone; ε_{max}, stress at break; σ_{max}, strain at break.

retro reaction, resulting in crack propagation.[85] This strategy has been used in the field of degradable polymers for >10 y, but research was mainly focused on shape-memory and/or reprocessable materials, with only recent interest in self-healing elastomers (Table 4).[86–88]

The first example reported by Rivero et al. was a DA-based elastomer obtained via the chain-end functionalization of PCL with furan and maleimide moieties.[89,90] They combined PCL-bearing furan/maleimide groups and PCL diol with hexamethylene diisocyanate (HDI) hard segments to produce self-healable PUs (Figure 5.2).[90] The elastomers exhibited E and ε_{max} values in the ranges 75–159 MPa and 200–540%, respectively, depending on the HDI content. This elastomer was limited in terms of self-healing, with only partial healing observed even after inducing the retro-DA reaction via heating to 100 °C (above the PCL melting temperature (T_m)) for 1 h and then maintaining the temperature at 50 °C for 24 h. A much-enhanced SHE was obtained for an elastomer based on bismaleimidic and bisfuranic PCL chains with urethane-thiourethane networks.[89] The elastomers exhibited E values of 20–350 MPa, depending on the content of the PCL cross-linker. At 60 °C (T_m of PCL), molecular rearrangements were promoted, and the healing time for scratches ranged from 2 to 72 h, depending on the PCL content. A faster and higher SHE was obtained at higher PCL contents, with SHEs of up to 91% in terms of E and σ_{max}.

5. Degradable Networks with Self-Healing Properties Based on Noncovalent Interactions/ Physical Bonds

The preceding sections discuss the various dynamic covalent bonds used to design self-healing, degradable/bioeliminable networks. In addition to this approach, self-healing networks may also be produced via noncovalent interactions, such as hydrogen bonds, hydrophobic, host-guest, electrostatic interactions, or metal coordination.

5.1. Hydrogen Bonds

Hydrogen bonding occurs between a hydrogen atom covalently bound to an electronegative atom, such as nitrogen, oxygen, or fluorine, and a lone pair of electrons of another electronegative atom. Although hydrogen bonds are largely present within hydrogels, only a few examples of hydrogels and elastomers based solely on hydrogen bonding with self-healing properties have been reported, and the data are shown in **Table 5**. As will be discussed in section V, hydrogen bonds are mostly combined with other mechanisms.

A recent example of a self-healing hydrogel involving only hydrogen bonds was reported by Ye et al.[91] These hydrogels were based on cytosine- and guanosine-modified HA and

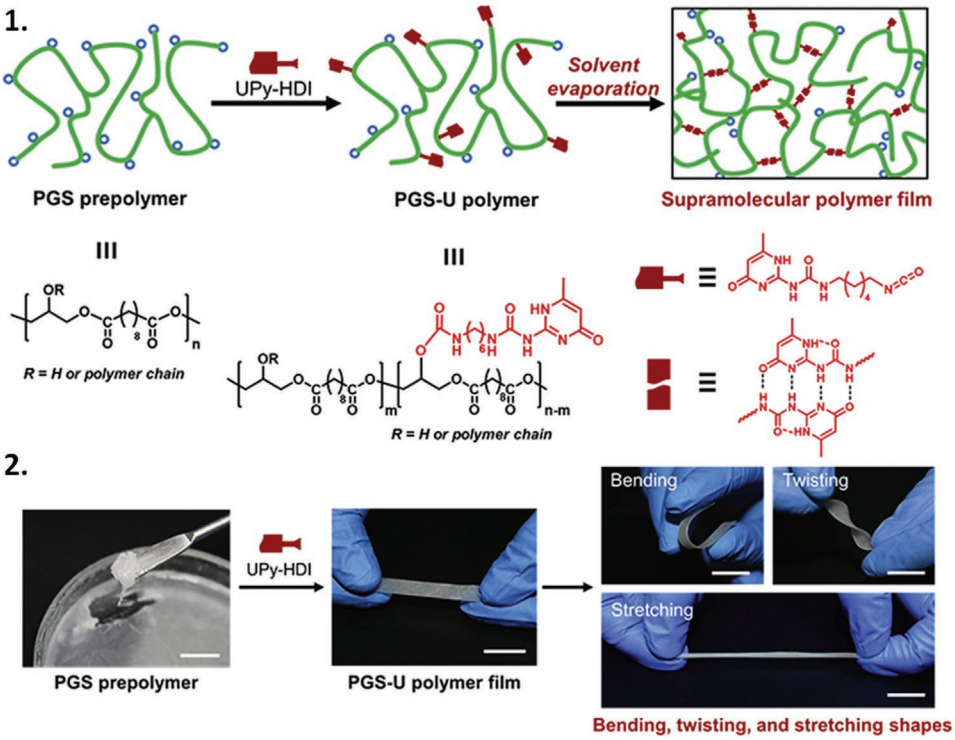

Figure 6. Synthesis of PGS-U polymers and preparation of supramolecular PGS-U film. 1) Schematic of PGS-U polymer synthesis and the supramolecular elastic film preparation by solvent evaporation. 2) Optical images of PGS prepolymer and supramolecular PGS-U film. Left: the viscous morphology of PGS prepolymer. Right: the bending, twisting, and stretching shapes of PGS-U polymer film. Scale bars: 20 mm. Adapted with permission.[98] Copyright 2016, Elsevier.

prepared via hydrogen bonding under physiological conditions, with 1,6-hexamethylenediamine as a bridging unit between the nucleobases and HA. G′ could be increased to 100 kPa, and self-healing was visually confirmed after 24 h. These hydrogels exhibited mass losses of ≈40% after 7 d in PBS solution in vitro. Hydrogels with identical healing times were prepared using BSA, with epichlorohydrin as the cross-linker.[92] The mechanical properties could be tuned as a function of the cross-linking density, with G′ ranging from 10 Pa to 4 kPa. The degradation was limited in PBS but could reach 70% in a trypsin solution after 72 h at 37 °C. Finally, cell viability assays using cancer cell lines confirmed the absence of hydrogel toxicity despite the use of epichlorohydrin.

For hydrogen bonding in elastomers, a commonly used chemical moiety is 2-ureido-4[1H]-pyrimidinone (UPy), which is a self-complementary quadruple hydrogen-bonding unit with a high dimerization constant and bonding strength (**Figure 6**). It is the focus of attention in the literature and used in biomedical applications, in particular as will be detailed in the last part of this review. To ensure degradability, three major degradable synthetic polymers have been used: polylactic acid (PLA), PCL, and poly(polyol-*co*-sebacate) (PPS). PLA-based elastomers were prepared using supramolecular assemblies of functional *α,ω*-UPy copolymers, including PLA-poly(ethylene-*co*-butylene)-PLA[93] or PLA-PEG-PLA.[94] In another strategy, PU with pending UPy units was prepared via the polycondensation of PLA diol, polytetrahydrofuran (PTHF), and a UPy-diol derivative in the presence of IPDI.[95] For the first two elastomers, *E* ranged from 4[93] to 900 MPa,[94] and self-healing times from 270 s[94] to 20 min [93] were observed with quantitative recoveries of *E*. In comparison, 24 h at a temperature of $>T_g$ was required to obtain a quantitative SHE in terms of σ_{max} for the last example.[95]

A dynamic network was obtained by grafting UPy into telechelic PTHF and 4-arm star-shaped PCL.[96] The resulting elastomers exhibited σ_{max} values of 3–8 MPa, and SHE could reach 88% with respect to σ_{max} after 48 h at 40 °C. A PCL-based reactive ink for use in digital light processing was formulated by combining dimethacrylate PCL macromonomers with methacrylates bearing UPy functionalities.[97] The 3D printed materials displayed *E* and σ_{max} values of 170 and ~11 MPa, respectively. At 80 °C, i.e., above the melting temperature of PCL, self-healing was visually realized after 1 h with a SHE of 80%.

Finally, regarding PPS, Wu et al. synthesized UPy-functionalized poly(glycerol-*co*-sebacate) (PGS) elastomers.[98] With an increase in the UPy concentration in the chain (from 16 to 33 wt.%), *E* increased from 0.4 to 33 MPa but the SHE decreased due to decreased chain mobility. Self-healing was realized visually at 55 °C after 60 min and mechanically after 12 h, as confirmed by the SHE with respect to σ_{max} of 85%. The enzymatic degradation of these PGS-based elastomers was studied, confirming a lower degree of degradation at the highest UPy content compared to those of UPy-free elastomers (59% vs 12% remaining mass after 84 h). Similar polymers and similar behaviors were reported by Chen et al. after grafting UPy into poly(sebacoyl diglyceride) (PSeD). The PSeD elastomers induced only a weak inflammation in vivo

Table 6. Self-healing hydrogels and elastomers based on hydrophobic, host-guest, or electrostatic/ionic interactions (materials, mechanical properties, SH evaluation, SH conditions, SHE, and degradation).

Nature	Mechanism	Materials	Mechanical properties	SH evaluation	SH conditions	SHE	Degradation	Ref.
Hydrogel	Hydrophobic interactions	Pentablock terpolypeptide	G' = 200 Pa to 8 kPa	–	< 15 s at 37 °C	100% (G')	In vitro, with leucine aminopeptidase and trypsin	[100]
Hydrogel	Hydrophobic interactions	Ferrocene-modified chitosan	G' = 1 kPa	Cut	4 h	100% (G')	–	[102]
Hydrogel	Hydrophobic interactions	Alginate, micelles of regenerated silk fibroin, and stearyl methacrylate	G' = 1 to 10kPa	Surface damage	12 h	100% (G')	In vitro, with protease XIV, no degradation in PBS	[103]
Hydrogel	Hydrophobic interactions	4-arm PEG-*b*-poly(γ-o-nitrobenzyl-L-glutamate)	G' = 2 kPa	Cut	5 min	100% (G')	Upon UV stimulation	[101]
Hydrogel	Host-guest interactions	HA-CD/HA-AD	G' = 50 to 400 Pa	–	–	100% (G')	In vitro, proteolytic	[104]
Hydrogel	Host-guest interactions	β-CD-modified PGA Cholesterol-modified triblock PGA-*b*-PEG-*b*-PGA	G' up to 20 kPa	Cut	60 s	–	In vitro, 36 d	[106]
Hydrogel	Host-guest interactions	β-CD-modified alginate/AD-modified graphene oxide	G' = 100 kPa	–	–	100% (G')	In vitro, 20 to 40% mass loss in 20 d	[105]
Hydrogel	Host-guest interactions	Poly(CD) Acrylamide N-vinyl-pyrrolidinone	E = 815 kPa	Cut	24 h, RT	98% (E)	In vitro, 28 to 35 h with β-lactamase	[107]
Hydrogel	Electrostatic/ionic interactions	Chitosan Carboxymethyl cellulose	G' = 500 Pa	Cut	12 h, RT	100% (G')	–	[108]
Elastomer	Electrostatic/ionic interactions	PCL diol modified with IPDI before chain extension with anionic oligo-alginate and cationic N-methyldiethanolamine	E = 19 to 93 MPa σ_{max} = 20 to 48 MPa ε_{max} = 800%	Cut	–	87% (toughness)	–	[109]

AD, adamantane; CD, cyclodextrin; E, Young's modulus; G', storage modulus; HA, hyaluronic acid; IPDI, isophorone diisocyanate; PCL, polycaprolactone; PGA, poly(L-glutamic acid); RT, room temperature; ε_{max}, strain at break; σ_{max}, stress at break.

28 d post-implantation in rats, which was comparable to the results observed using the poly(lactic-*co*-glycolic acid) (PLGA) control.[99]

5.2. Hydrophobic Interactions

Hydrophobic interactions are reversible and noncovalent and occur between non-polar hydrophobic groups immersed in aqueous media. Non-polar substances generally aggregate to minimize their contact with water. Numerous classical physically cross-linked hydrogels are based on hydrophobic interactions and by nature, they could be considered self-healable. However, in this review, we only analyze the most recent examples of such hydrogels claiming self-healing properties (**Table 6**).

These examples rely on interactions between the hydrophobic groups of the (co)polymer chain, such as benzyl,[100] photolabile *o*-nitrobenzyl,[101] and ferrocene groups,[102] e.g., Bilalis et al. mixed a poly(lysine)-*b*-poly(L-histidine-*co*-γ-benzyl-L-glutamate)-*b*-poly(lysine)-*b*-poly(L-histidine-*co*-γ-benzyl-L-glutamate)-*b*-poly(lysine) pentablock copolymer with an aqueous solution of gemcitabine to prepare hydrogels with G' values of 200 Pa–8 kPa and very fast self-healing times of 15 s.[100] Another strategy involving hydrophobic interactions with micelles was proposed by Meng et al..[103] They prepared micelles of amphiphilic regenerated silk fibroin containing the hydrophobic monomer stearyl methacrylate in an alginate network physically cross-linked with calcium ions. Owing to the hydrophobic interactions used as sacrificial bonds, the rupture energy could be efficiently dissipated while ensuring the reversibility of the interactions, a higher modulus (≈ 400 Pa), and self-healing within 12 h after damage.

5.3. Host-Guest Interactions

Host-guest interactions occur via mutual molecular recognition of "host" and "guest" moieties. The host moieties are macrocyclic molecules wherein the guest moiety may be inserted to form a unique inclusion complex. One important molecule used to form host-guest interactions in the examples reported in the recent literature is cyclodextrin (CD), as shown in Table 6. Two strategies are used to exploit the CD moieties. First, CD may be used as a functional group on the polymer backbone. This approach is largely used in preparing supramolecular shear-thinning, self-healing hydrogels based on the host-guest interactions between HA modified with adamantane (AD) and CD,[104] β-CD-modified alginate and AD-modified graphene oxide,[105] or β-CD-modified poly(L-glutamic acid) (PGA) and cholesterol-modified triblock PGA-*b*-PEG-*b*-PGA.[106] The second strategy relies on the use of polycyclodextrin. An example was reported by Yu et al. with a host backbone comprising polycarboxymethyl-β-CDs, a β-lactam-sensitive bifunctional AD guest molecule, and to reinforce the network, an

Table 7. Self-healing hydrogels based on metal-coordination (materials, mechanical properties, SH evaluation, SH conditions, SHE, and degradation).

Nature	Materials	Mechanical properties	SH evaluation	SH conditions	SHE	Degradation	Ref.
Hydrogel	PAA Polypyrrole Fe^{3+}	σ_{max} = 0.52 to 0.83 MPa ε_{max} = 180 to 448%	Cut	12 h, 37 °C	74% (σ_{max})	–	[110]
Hydrogel	CMC EDTA:Fe^{3+} Silver nanoparticles	G' = 700 to 800 Pa	Cut	1min	–	–	[112]
Hydrogel	PAA Chitosan Fe^{3+}	σ_{max} = 3.7 MPa ε_{max} = 1200%	Cut	24 h, 70 °C	38% (σ_{max}) 58% (ε_{max})	–	[111]
Hydrogel	CMC Fe^{3+}/Al^{3+}	G' = 2 kPa	Cut	1 min, RT	100% (G')	–	[113]
Hydrogel	CMC PCAD Al^{3+}	E = 3. To 16.8 kPa σ_{max} = 5.1 to 12.9 kPa ε_{max} = 90 to 280%	Cut	12 to 24 h, RT	92% (σ_{max}) 95% (ε_{max})	–	[114]
Hydrogel	Polyaspartamide/histamine conjugate Cu^{2+}	G' up to 10 kPa	Cut	5 h, water	–	–	[115]
Hydrogel	Thiolated BSA Silver nitrate	G' = 400 Pa	Cut	–	100% (G')	–	[116]
Hydrogel	Histidine peptide Zn^{2+}	E = 15 kPa ε_{max} = 620%		1 h	100% (G')	–	[117]

BSA, bovine serum albumin; CMC, carboxymethyl chitosan; G', storage modulus; PAA, poly(acrylic acid); PCAD, photoluminescent citric acid derivatives; ε_{max}, strain at break; σ_{max}, stress at break.

interpenetrating network polymerized via acrylamide and *N*-vinylpyrrolidinone.[107] Depending on the system, soft (G' < 500 Pa) [104] or strong (G' > 100 kPa) [105,107] gels are formed, with the stronger gels obtained owing to the hybrid natures of those with embedded particles or the reinforcing effects of the interpenetrating networks. In all cases, they exhibited quantitative SHEs after repair times ranging from a few seconds [106] to one day.[107] Complete degradation of these host-guest hydrogels was ensured via enzymatic degradation by collagenases, matrix metalloproteinases,[104] or β-lactamases,[107] although simple hydrolytic degradation was also reported.[105,106]

5.4. Electrostatic/Ionic Interactions

Electrostatic or ionic interactions occur between ions with opposite charges and may be used to produce self-healing hydrogels. However, similar to hydrophobic interactions, although these interactions are commonly used to yield polyelectrolyte-based hydrogels, only a few examples have been reported in the recent literature (Table 6).

Electrostatic interactions between positively charged chitosan and negatively charged carboxymethyl cellulose have been exploited.[108] When cut into two pieces, the samples displayed self-repair times of 12 h at room temperature. Healing was confirmed via SEM and rheological studies, with the healed hydrogels displaying G' values close to the original value (500 Pa). Regarding elastomers, Baharvand et al. focused on biodegradable elastomers engineered via supramolecular ionic interactions. To enhance the strengths of the biodegradable elastomers, they used a PCL diol that was further modified with IPDI before chain extension with anionic oligo-alginate or cationic *N*-methyldiethanolamine.[109] This synthetic pathway yielded PU networks with ionic interactions between the PU chains, resulting in elastomers with high elastic contributions. The highest G' values were observed for networks with 1:1 ratios of cationic and anionic segments, with E and σ_{max} values of up to 93 and 48 MPa, respectively, and ε_{max} values of ≈ 800%. Their degrees of self-healing was estimated by measuring their toughnesses, yielding SHEs of 87%.

5.5. Metal Coordination

The use of reversible metal coordination interactions is another method of producing self-healing hydrogels via dynamic physical bonding, and several recent examples are shown in **Table 7**.

Although different metals may be used, Fe^{3+} is the most widely employed. Fe^{3+}-coordination interactions enable self-healing, but with discrepancies in terms of SHE and repair time ranging from 1 min to 1 d. For example, slow repair times (>12 h) and limited SHEs were observed for hydrogels composed of polyacrylic acid (PAA) and Fe^{3+} ions, with the highest SHE of 74% observed when mixed with polypyrrole,[110] and a SHE of only 38% observed when mixed with chitosan.[111] This limited self-healing may be due to the high mechanical properties of the systems, which exhibit remarkable σ_{max} values for hydrogels in the megapascal range, traducing the strength of the initial network. In contrast, the use of Fe^{3+} with CMC yielded softer hydrogels that displayed faster full repair.[112,113]

Table 8. Self-healing hydrogels and elastomers based on combination of dynamic chemical bonds (materials, mechanisms, mechanical properties, SH evaluation, SH conditions, SHE, and degradation).

Nature	Mechanism	Materials	Mechanical properties	SH evaluation	SH conditions	SHE	Degradation	Ref.
Hydrogel	Schiff base Acylhydrazone bonds	Gelatin A-Alg Adipic acid dihydrazide	G' = 20 kPa	Cut	Moisture	100% (G')	In vitro, with collagenase, 70% mass loss after 20 d	[118]
Hydrogel	Schiff base Acylhydrazone bonds	Gelatin A-Dex Adipic acid dihydrazide bFGF@PLGA Chlorhexidine acetate	G' = 600 Pa to 1.8 kPa	Cut, Hole	1 h	–	In vitro, 50 h	[119]
Hydrogel	Schiff base Boronate ester bonds	PEG-BA Phenylboronic acid-PEG PVA Glycol chitosan	G' up to 5.7 kPa	Syringe injection	1 h	98% (G')	–	[120]
Hydrogel	Schiff base Boronate ester bonds	Gelatin/A-Alg Borax	G' = 1 kPa	Cut	7 d	80% (G')	–	[121]
Hydrogel	Schiff base Boronate ester bonds	Gelatin/Dialdehyde dextrin Dialdehyde carboxymethylcellulose Borax Glutaraldehyde	–	Cut	4 h, pressure	-	In vitro, 1 week	[122]
Elastomer	DA Disulfide bonds	Polyurethane (HDI) with PCL	E = 0.1 MPa σ_{max} up to 33 MPa	Scratch	60 °C, then 120 °C, then RT	113% (σ_{max})	–	[123]

A-Alg, aldehyde-modified alginate; A-Dex, aldehyde-modified dextran, bFGF@PLGA, PLGA microspheres integrated with a basic fibroblast growth factor; E, Young's modulus; G', storage modulus; HDI, hexamethylene diisocyanate; PCL, polycaprolactone; PEG, poly(ethylene glycol); PEG-BA, benzaldehyde poly(ethylene glycol); PVA, poly(vinyl alcohol); RT, room temperature; σ_{max}, stress at break.

In addition to Fe^{3+}, other metal ions, including Al^{3+},[114] Cu^{2+},[115] Ag^{+},[116] and Zn^{2+},[117] have been used. For example, Moon et al.[115] reported the syntheses of biodegradable polyaspartamide derivatives conjugated with histamine to prepare a metal-coordinated supramolecular hydrogel with Cu^{2+} metal ions in an aqueous solution that displayed the capacity to heal in 5 h, with a G' of ≈10 kPa. Thiolated BSA and silver nitrate have also been used to produce an injectable, self-healing, antibacterial BSA-based hydrogel for use in bone regeneration.[116] The resulting hydrogel was softer than the previous one, with a G' of ≈400 Pa and shear-thinning behavior, enabling its rapid recovery.

6. Degradable Networks with Self-Healing Properties Based on Multi-Mechanisms

The aforementioned examples of degradable self-healing hydrogels and elastomers rely on single self-healing mechanisms. However, self-healing may also be caused by a combination of various dynamic chemical bonds, various physical interactions, or a combination of chemical bonds and physical interactions. Owing to the complexity of designing such materials, this approach has been mainly applied to dual-self-healing mechanisms, although degradable networks with more than two self-healing mechanisms are also described in this section. The selection of mechanisms associated with the optimal properties depends mainly on the desired application. Generally, to increase Young's modulus or elasticity of the material, higher contents of reversible covalent linkages are preferred, whereas to favor more spontaneous self-healing without depending on external stimuli, physical dynamic bonds should be selected.

6.1. Dual Self-Healing via the Combination Of Dynamic Chemical Bonds

Five examples of degradable self-healing hydrogels with combinations of dynamic chemical bonds have recently been reported and are summarized in **Table 8**. In the first two cases, the networks are based on dynamic Schiff base reactions and acylhydrazone bonds in similar systems, relying on gelatin, adipic acid dihydrazide, and A-Alg [118] or A-Dex [119] (**Figure 7**.1). To enhance the antibacterial activity and accelerate wound healing, microspheres of PLGA loaded with basic fibroblast growth factor (bFGF@PLGA) and chlorhexidine acetate (CHA) were embedded in soft gels (typical G' values of 600 Pa–1.8 kPa) that self-repaired after 1 h and could be fully degraded in PBS after 50 h.

Notably, these systems, based on dextran or alginate, displayed good biocompatibilities in vitro and in vivo. In another example, self-healing was based on dynamic imine bonds associated with borate ester linkages.[120] The system was composed of multifunctional benzaldehyde- and phenylboronic acid-modified PEG cross-linked with PVA and glycol chitosan. Regarding the self-healing capacity, even the stiffer sample (G' = 5.7 kPa) could recover after 45 min post-injection, with a SHE of 98%.

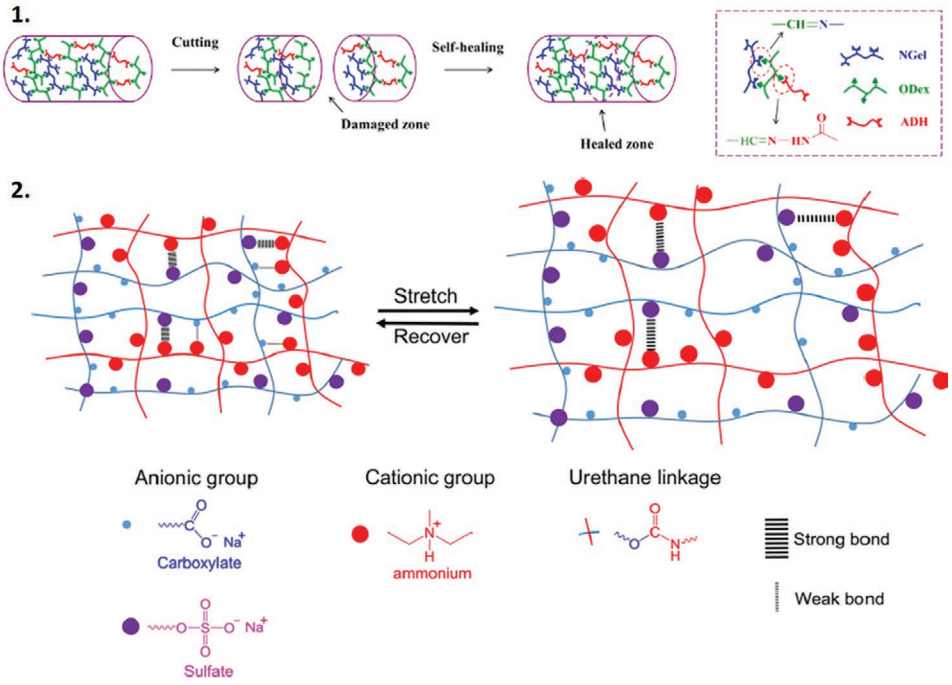

Figure 7. 1) Schematic representation of the self-healing mechanism based on Schiff base and acylhydrazone bonds. 2) Schematic presentations of dual physically cross-linked supramolecular elastomers composed of ionic networks with different strengths. The strong bonds (soft tertiary ammonium-soft sulfate pairs) and weak bonds (soft tertiary ammonium-hard carboxylate groups) act as reversible sacrificial bonds under deformation. Adapted with permission.[119,130] Copyright 2019, Elsevier. Copyright 2021, Elsevier.

Other examples include gelatin that was associated with A-Alg and borax [121] or dialdehyde dextrin and dialdehyde carboxymethyl cellulose with borax and glutaraldehyde,[122] which exhibited slow (7 d) and fast (4 h) self-healing, respectively.

Wang et al. designed a dual self-healing PU elastomer based on DA adducts and disulfide bonds as self-repairing coatings with shape-memory properties.[123] The PU was prepared using diols containing DA bonds, PCL-diol, and HDI. The PU prepolymer was further cross-linked with trimethylolpropane tris(3-mercaptopropionate). σ_{max} reached 33 MPa and G' was close to 0.1 MPa, with a SHE of 113%. Self-healing was realized in three phases: heating at 60 °C to enable the melting of PCL and reduce the scratch, heating at 120 °C to activate the retro-DA reaction, and the final DA reaction occurred after cooling to room temperature.

6.2. Dual Self-Healing via the Combination of Physical Interactions

Compared with the limited number of examples combining two types of dynamic bonds, numerous self-healing hydrogels are based on multiple physical interactions, and the main combinations are listed in this section and **Table 9**.

6.2.1. Combination of Hydrogen Bonds and Hydrophobic Interactions

The combination of hydrophobic interactions and hydrogen bonding is illustrated here using three recent examples. The first hydrogel relied on polyglycerol sebacate-polyethylene glycol methyl ether methacrylate copolymers associated with α-CD.[124] Another synthetic hydrogel was obtained by polymerizing gelatin methacrylate with 2-(2-methoxyethoxy)ethyl methacrylate to produce a hybrid branched copolymer.[126] Both hydrogels displayed the capacity to recover after shear thinning. However, they differed in terms of degradation, with the first exhibiting stability over 2 months at neutral pH and requiring acidic or basic conditions to degrade. Conversely, the second could be enzymatically degraded in the presence of collagenase after 36 h in vitro and 2–3 months in vivo. In terms of natural polymers, denaturation of BSA via thermal treatment has been proposed.[125] Denaturation leads to changes in the protein conformation and the exposure of hydrophobic groups initially concealed in the protein core to enable hydrophobic interactions in parallel to hydrogen bonding, resulting in a SHE in terms of σ_{max} of 100% after 1 h.

6.2.2. Combination of Hydrogen Bonds and Electrostatic/Ionic Interactions

Natural polymers are key in preparing degradable networks that combine hydrogen bonding and electrostatic interactions. A gelatin-based electroconductive soft hydrogel was prepared using cross-linked gelatin functionalized with carboxylated multi-walled carbon nanotubes (CNTs) and PEDOT:PSS (mix of poly(3.4-ethylenedioxythiphene) and polystyrene sulfonate).[127] A chitosan-based hydrogel was synthesized via in situ free-radical polymerization of acrylic acid and acrylamide in the presence of chitosan in a dilute aqueous acetic

Table 9. Self-healing hydrogels and elastomers based on a combination of physical interactions (materials, mechanism, mechanical properties, SH evaluation, SH conditions, SHE, and degradation).

Nature	Mechanism	Materials	Mechanical properties	SH evaluation	SH conditions	SHE	Degradation	Ref.
Hydrogel	Hydrogen bonds Hydrophobic interactions	Polyglycerol sebacate -PEG methyl ether methacrylate α-CD	G' = 1 to 100 kPa	–	–	–	In vitro, in acidic or basic environments	[124]
Hydrogel	Hydrogen bonds Hydrophobic interactions	Denatured BSA	σ_{max} = 60 kPa	Cut	60 min, 80 °C	100% (σ_{max})	In vivo	[125]
Hydrogel	Hydrogen bonds Hydrophobic interactions	Gelatin methacrylate 2-(2-methoxyethoxy) ethyl methacrylate	G' = 1 to 400 Pa	Scratch	90 min, 37 °C	100% (G')	In vitro, 100% mass loss with collagenase in 36 h In vivo, 100% degradation after 56 to 84 d	[126]
Hydrogel	Hydrogen bonds Electrostatic/ionic interactions	Gelatin EDC PEDOT:PSS MWCNTs-COOH	G' = 4 to 11 kPa	Cut	10 min	100% (Visual)	In vitro, 90 to 100% degradation in 20 d	[127]
Hydrogel	Hydrogen bonds Electrostatic/ionic interactions	Poly(acrylic acid-co- acrylamide) Chitosan	G' = 0.2 to 1 kPa	Cut	1 d	88% (σ_{max})	In vitro, acidic conditions	[128]
Hydrogel	Hydrogen bonds Electrostatic/ionic interactions	Starch PVA Borax	ε_{max} = 2500% Toughness = 290 kJ m^{-3} Compression strength = 550 kPa	Cut	600 s	69% (σ_{max}) 81% (ε_{max})	–	[129]
Elastomer	Hydrogen bonds Electrostatic/ionic interactions	Polyurethane (PCL/HDI) Sulfated alginate	E = 0.9 to 7.7 MPa σ_{max} = 2 to 8.7 MPa Toughness = 61 MJ m^{-3}	Cut	5 min, RT	100%	–	[130]
Hydrogel	Hydrogen bonds Metal-coordination	Poly(acrylic acid-*co*-acrylamide) PVA Fe^{3+} Borax	G' = 1 to 10 kPa	Cut	48 h, 40 °C	85% (σ_{max})	In vitro, 3 to 70% mass loss in 10d	[131]
Hydrogel	Hydrogen bonds Metal-coordination	Poly(glycerol sebacate)-*co*-poly(ethylene glycol)-*g*-catechol Fe^{3+} UPy-functional gelatin	G' = 2 kPa	Cut Hole	< 12 min at 37 °C 45 s under NIR irradiation	–	In vitro, 7 to 10d	[132]
Elastomer	Hydrogen bonds Metal-coordination	Poly(δ-valerolactone)-*co*-poly(lactic acid) containing UPy bpy	Fracture energy up to 80 MJ.m^{-3}	Scratch	30 min, 50 °C	77% (Visual)	–	[133]
Hydrogel	Hydrophobic interactions Metal-coordination	κ-carrageenan PAA Zr^{4+} D-galactose Micelles of n-octadecyl acrylate dissolved in sodium dodecyl sulfate	σ_{max} = 2.5 Mpa ε_{max} = 1382% Toughness = 13.4 MJ m^{-3}	Cut	24 h, 70 °C	67% (toughness)	In vitro, 27 to 47% mass loss after 24d	[134]
Hydrogel	Miscellaneous interactions	Proline-rich peptide-PEG copolymer, recombinant linear protein, and PNIPAM	G' = 100 Pa	–	–	100% (G')	In vitro, 70% degradation after 14d	[135]

BSA, bovine serum albumin; CD, cyclodextrin; E, Young's modulus; EDC, N-(3-dimethylamino-propyl)-N'-ethylcarbodiimide hydrochloride; G', storage modulus; HDI, hexamethylene diisocyanate; MWCNTs, multi-walled carbon nanotubes; PCL, polycaprolactone; PEG, poly(ethylene glycol); PVA, poly(vinyl alcohol); σ_{max}, stress at break.

acid solution.[128] The resulting hydrogel was composed of poly(acrylic acid-*co*-acrylamide) copolymers grafted onto chitosan chains and a small proportion of nongrafted chains that could interact via multiple noncovalent interactions. Finally, a stretchable (ε_{max} of 2500%), strong (compression strength of 550 kPa) starch/PVA/borax hybrid dual-cross-linked hydrogel

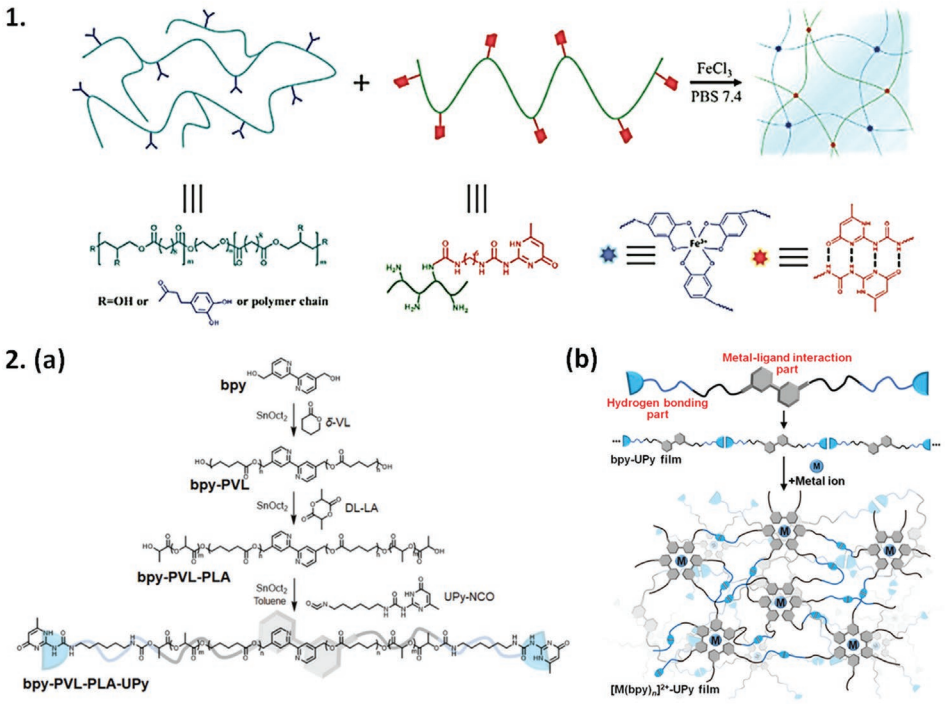

Figure 8. 1) Schematic diagram of the dual dynamic cross-linking based on hydrogen bonds and catechol-Fe coordination in the hydrogel network. 2) a) Preparation of bpy-PVL-PLA-UPy b) Schematic illustration of the bpy-UPy and $([M(bpy)n]^{2+}$-UPy film. Adapted with permission.[132,133] Copyright 2020, Wiley-VCH. Copyright 2019, Royal Society of Chemistry.

was developed.[129] These hydrogels displayed rapid self-healing capacities, with repair times ranging from a few seconds to 1 h.

Only one dual self-healable elastomer with this combination of interactions was reported by Baharvand et al. Based on their previous studies regarding alginate-based supramolecular PU based on PCL,[109] they introduced dual cross-linking via chain-end functionalization using sulfated alginate,[130] enabling strong and weak ionic interactions between tertiary ammonium and sulfate or carboxylate groups, respectively (Figure 7.2). The dual physically cross-linked elastomers exhibited SHEs of 100% after 5 min at room temperature, with high toughnesses and mechanical properties close to those of vascular tissues (*E* values of 1–8 MPa).

6.2.3. Combination of Hydrogen Bonds and Metal-Coordination Interactions

Biodegradable double-network hydrogels composed of biodegradable poly(acrylic acid-*co*-acrylamide)/PVA and involving metal coordination were developed by Jing et al..[131] The ionic coordination between the carboxylate groups and Fe^{3+} and hydrogen bonding between the carboxylic and amide groups formed the first network, whereas the second was based on the complexation between PVA and borax. The resulting hydrogel exhibited a G' of 1–10 kPa, and the SHE in terms of σ_{max} reached 85% after 48 h at 40 °C. After 10 d in PBS and simulated intestinal fluid, a mass loss of up to 70% was measured as a function of the acrylamide content. In another study, Zhao et al.[132] designed an injectable dual-network self-healing hydrogel combining poly(glycerol sebacate)-*co*-PEG-*g*-catechol to yield catechol-Fe^{3+} coordination cross-links and UPy-functionalized gelatin to yield quadruple hydrogen bonding cross-links (**Figure 8**.1). G' was ≈ 1 kPa at 37 °C, and the hydrogel could heal at body temperature in 12 min and even 45 s under heating via near-IR irradiation. In PBS, the hydrogels exhibited linear mass losses and were completely degraded after 10 d.

An elastomer with dual self-healing properties and displaying hydrogen-bonding and metal-ligand interactions was developed using a poly(δ-valerolactone)-*co*-PLA copolymer containing UPy, 2,2-bipyridine, and Fe^{2+}, Co^{2+} or Zn^{2+} ions (Figure 8.2).[133] With dual-cross-linking, the fracture energy, which reached 80 MJ m^{-3}, was a function of the cation in the order $Fe^{2+} > Co^{2+} > Zn^{2+}$. Using the scratch method, visual healing was realized after 30 min at 50 °C with a SHE of 77% for metal-UPy, whereas the SHE of the pure UPy under the same conditions was only 51%.

6.2.4. Other Combinations of Physical Interactions

Zhao et al. [134] prepared a κ-carrageenan/PAA double-network hydrogel based on metal coordination and hydrophobic interactions. The first network was composed of κ-carrageenan chains and Zr^{4+} cations that interacted with D-galactose. The second interpenetrated network was based on PAA and associated with hydrophobic micelles of *n*-octadecyl acrylate dissolved in sodium dodecyl sulfate. After cutting, samples placed in contact for 24 h at 70 °C could heal and withstand large deformations (~400%) without breakage, whereas the

toughness recovery was 67% after 2 min. The biodegradability was investigated in vitro in PBS and evaluated via the loss of mechanical properties (close to zero after 24 h) and mass (27–47% after 24 d).

Cai et al. [135] designed soft hydrogels with maximum G' values of ≈ 100 Pa with two physical cross-linking mechanisms: weak heterodimeric *ex vivo* molecular recognition and in vivo cross-linking due to the thermo-responsive formation of a reinforcing network. The first network was composed of a star-shaped proline-rich peptide-PEG copolymer assembled with a recombinant linear protein bearing CC43 WW and RGD cell-binding domains connected by hydrophilic spacers. The second was based on PNIPAM chains conjugated to the PEG copolymer, and the erosion of the material was ~70% after 14 d in vitro.

6.3. Dual Self-Healing via a Combination Of Dynamic Chemical Bonds and Physical Interactions

6.3.1. Combination of Schiff-base and Physical Interactions

Unsurprisingly, due to the numerous self-healing systems relying on Schiff-base reactions, this dynamic bond is the most common one in dual self-healing systems combining dynamic chemical bonds and physical interactions. Several examples of self-healing hydrogels based on the combination of dynamic Schiff-base bonds as the chemical bonds and copolymer micelle cross-linking as the physical interactions have been reported (**Table 10**). Guo et al. [136] prepared hydrogels by mixing quaternized chitosan with micelles of benzaldehyde-terminated Pluronic F-127 (PF-127) under physiological conditions. Similarly, hydrogels based on CEC and benzaldehyde-terminated PF-127/CNTs were prepared.[137] Self-healing was due to the Schiff-base and physical cross-linking interactions of the PF-127 micelles and CNTs. In both examples, the self-healing times were 2–3 h and the G' values were in the range of 10–30 kPa.

Other dual self-healing hydrogels combine Schiff-base bonds and catechol-Fe coordination. This is the case for catechol-modified poly(L-lysine) and A-Dex [138] or catechol-modified oxidized HA and aminated gelatin,[139] which are associated with Fe^{3+} ions. The first system yielded soft gels with G' values limited to 7.6 kPa compared to the G' of the second system of 535 kPa. The hydrogels rapidly self-healed with SHEs of >91% and could degrade in PBS or in the presence of iron-chelating competitors. The cytocompatibility of the catechol-modified poly(L-lysine)/A-Dex hydrogel was confirmed toward L929 and NIH 3T3 murine cells.

Finally, Schiff-base linkages were also combined with host-guest interactions [140] or hydrogen bonds.[141] This is exemplified by hydrogels composed of the guest polymer, phenolphthalein-grafted CEC, the host molecule, hexamethylenediamine-modified β-CD, and A-Alg,[140] or chitosan hydrogels cross-linked with vanillin.[141] In the latter case, the amino group of chitosan could react with the aldehyde group of vanillin via a Schiff-base reaction, and its hydroxyl groups could form hydrogen bonds with the hydroxyl or amino groups of another chitosan chain. For these two types of hydrogels, repair times of a few hours were required to reach SHEs of ≥80%.

6.3.2. Dual-self-healing systems: other combinations

Two recent examples based on hydrogen bonds and boronate esters are reported in the literature (Table 10). The first was composed of PVA, borax, and carboxymethyl cellulose.[142] In this case, σ_{max} and E could reach 720 and 340 kPa, respectively, and self-healing was realized after 16 h at 20 °C. In the second example, hydrogels were obtained using dynamic benzoxaborole-sugar interactions and quadruple hydrogen bonds of UPy moieties in poly(DMA-*st*-META-*st*-LAEMA) and poly(MPC-*st*-UPyHEMA-*st*-MAABO) copolymers.[143] Depending on the compositions of the different gels, G' ranged from 0.3 to 1.1 kPa. Self-healing times were rapid, with shape recoveries in only 20 s for the samples evaluated via the cutting method.

Disulfide bonds have also been used in systems with hydrogen bonds. Wen et al. proposed a degradable PU hydrogel composed of PCL, PEG, and IPDI, containing disulfide bonds and hydrogen bonds.[144] The SHE, as quantified via tensile test reached 97%, and the materials exhibited high mechanical strengths, with σ_{max} values of up to 3.3 MPa. At all PU/PCL ratios, the mass loss in PBS was limited to 8% after 30 d.

A combination of DA adducts and electrostatic interactions was proposed by Li et al., using pectin/chitosan hydrogels. Pectin was modified with furfural to form the conjugated diene partner, and 6-maleidocaproic acid was grafted onto chitosan to yield the dienophile partner.[145] The hydrogels healed in 5 h at 37 °C and could bear a mass of 5 N without damage.

Finally, Jiang et al. imparted self-healing properties on elastomers due to oxime-urethane and hydrogen bonds.[146] PU copolymers based on dimethylglyoxime, IPDI, PTHF, and glycerol were prepared. Depending on the glycerol content, σ_{max}, E, and ε_{max} values of 33 kPa–4.4 MPa, 172 kPa–3.7 MPa, and 500–3300%, respectively, were obtained. The self-healing capacity was also a function of the glycerol content. After healing at room temperature for 5 min, the SHEs in terms of σ_{max} were >80% for elastomers but limited to 37% at low and high glycerol contents. Under in vitro enzymatic conditions, the elastomers lost 7.5% of their masses after nine days.

6.4. Multi-mechanism self-healing systems

Finally, although uncommon, the self-healing properties may be due to the combination of more than two mechanisms. To the best of our knowledge, only two examples have combined two types of chemical linkages with one physical interaction. In both cases, boronate ester bonds are associated with Schiff-base linkages and hydrogen bonds [147] or electrostatic interactions.[148] In the first system, hydrogels were prepared using PVA and borax as the matrix, which was reinforced with cellulose nanofibers and dopamine-grafted oxidized carboxymethyl cellulose. In the second study, gels were prepared using borax-functionalized oxidized chondroitin sulfate (BOC), gelatin, and BOC-doped polypyrrole. Both hydrogels were cytocompatible in vitro and exhibited similar healing times of ≈ 5 min and G' values in the range of 0.4–10 kPa.

A combination of two physical interactions and one chemical reversible bond is also possible. This is the case in a study by Tran et al. [149] that reported hydrogels based on dynamic

Table 10. Self-healing hydrogels and elastomers based on combination of dynamic chemical bonds and physical interactions (materials, mechanisms, mechanical properties, SH evaluation, SH conditions, SHE, and degradation).

Nature	Mechanism	Materials	Mechanical properties	SH evaluation	SH conditions	SHE	Degradation	Ref.
Hydrogel	Schiff base Copolymer micelle cross-linking	Quaternized chitosan Benzaldehyde-terminated Pluronic micelles	E = 21 to 37 kPa G' = 22 to 53 kPa	Cut	2 h, 25 °C	100% (G')	In vitro	[136]
Hydrogel	Schiff base Cross-linking interactions of micelles and CNTs	CEC Benzaldehyde Pluronic micelles CNTs	G' = 6 to 16 kPa	Cut	3 h	100%	In vitro, 49 to 74% mass loss in 13d	[137]
Hydrogel	Schiff base Catechol-Fe coordination	Catechol modified poly(L-lysine) A-Dex Fe	G' = 0.7 to 7.6 kPa Compression stress = 25 to 80 kPa	Cut	Water	91%	In vitro, with deferoxamine mesylate	[138]
Hydrogel	Schiff base Catechol-Fe coordination	Catechol-modified oxidized HA Aminated gelatin Fe^{3+}	G' up to 535 kPa	Cut Syringe injection	15 min	97% (G')	In vitro, 12d	[139]
Hydrogel	Schiff base Host-guest interactions	Phenolphthalein-grafted CEC Hexamethylenediamine modified β-CD A-Alg	Compression stress up to 12.5 kPa	Cut	4 h	80%	In vitro, 54 to 66% mass loss in 168h	[140]
Hydrogel	Schiff base Hydrogen bonds	Chitosan Vanillin	G' up to 80 kPa	Cut	5 h	93% (σ_{max}) 99% (ε_{max})	–	[141]
Hydrogel	Boronate ester bonds Hydrogen bonds	PVA Borax Carboxymethylcellulose	E up to 340 kPa σ_{max} up to 760 kPa	Cut	16 h, 20 °C	80% (σ_{max})	–	[142]
Hydrogel	Boronate ester bonds Hydrogen bonds	Poly(DMA-*st*-META-*st*-LAEMA) Poly (MPC-*st*-UPyHEMA-*st*-MABBO)	G' = 0.3 to 1.1 kPa	Cut	20 s	100% (G')	In vitro, 120 min with fructose	[143]
Hydrogel	Disulfide bonds Hydrogen bonds	PU (IPDI) — PCL—PEG	σ_{max} = 3.3 MPa	Cut	10 min at 50 °C, then 1 h at RT and 24 h in water	97% (σ_{max})	In vitro, 4 to 8% mass loss in 30 d	[144]
Hydrogel	DA bonds Electrostatic interactions	Furfural-pectin 6-maleidocaproic acid chitosan	–	Cut	5 h, 37 °C	–	–	[145]
Elastomer	Oxime-urethane bonds Hydrogen bonds	PU based on dimethylglyoxime, IPDI, PTMEG, and glycol	E = 172 kPa to 3.7 MPa σ_{max} = 33 kPa to 4.4 MPa ε_{max} = 500 to 3300%	Cut	5 min, RT	80% (σ_{max})	In vitro, 7.5% mass loss with enzyme after 9d	[146]
Hydrogel	Boronate ester bonds Schiff base Hydrogen bonds	PVA Borax Cellulose nanofibers Dopamine-grafted oxidized carbomethyl cellulose	G' = 2 to 10 kPa	Cut	5 min	100% (G')	In vitro, pH-dependent, up to 60% mass loss in 3.5 h at pH 5	[147]
Hydrogel	Boronate ester bonds Schiff base Electrostatic interactions	BOC Gelatin BOC-doped polypyrrole	G' = 0.4 to 1.6 kPa	Cut	5min	–	In vivo, 14 to 21d	[148]
Hydrogel	Disulfide bonds Hydrogen bonds Ionic interactions	2,3-dimercapto-1-propanol Meso-2,3-dimercaptosuccinic acid Ca^{2+}	E = 13.4 kPa σ_{max} 12.1 kPa ε_{max} = 4334%	Cut	1 min, 25 °C, air or water	93 to 100% (E, σ_{max}, ε_{max})	In vitro, 5 h with glutathione	[149]

Table 10. Continued.

Nature	Mechanism	Materials	Mechanical properties	SH evaluation	SH conditions	SHE	Degradation	Ref.
Hydrogel	Boronate ester Hydrogens bonds Hydration	Guar gum-*g*-poly(acrylamidoglycolic acid) Silver nitrate Sodium borohydride	Compression (module 0.043 to 0.112 MPa; strain = 80 to 89%)	Cut Syringe injection	25 °C	–	–	[150]

A-Alg, aldehyde-modified alginate; A-Dex, aldehyde-modified dextran; BOC, borax-functionalized oxidized chondroitin sulfate; CD, cyclodextrin; CEC, carboxyethyl chitosan; CNTs, carbon nanotubes; DMA, *N*-*N*-dimethylacrylamide; *E*, Young's modulus; *G′*, storage modulus; HA, hyaluronic acid; HEMA, 2-hydroxyethyl methacrylate; IPDI, isophorone diisocyanate; LAEMA, 2-lactobioamidoethyl methacrylamide; MAABO, 5-methacrylamido-1,2-benzoxaborole; META, [2-(methacryloyloxy)ethyl] trimethylammonium chloride; MPC, 2-methacryloyloxyethyl phosphorylcholine; PCL, polycaprolactone; PEG, poly(ethylene glycol); PTMEG, poly(tetramethylene ether)glycol; PU, polyurethane; PVA, poly(vinyl alcohol); RT, room temperature; ε_{max}, strain at break; σ_{max}, stress at break.

poly(disulfide) backbones and rapidly reversible physical cross-links, such as hydrogen bonds and ionic interactions (**Figure 9**). They copolymerized 2,3-dimercapto-1-propanol and meso-2,3-dimercaptosuccinic acid before generating hydrogels in aqueous Ca^{2+} solutions. These hydrogels immediately reconnected after cutting and exhibited rapid self-healing in air at 25 °C or water. The quantitative SHE was confirmed via mechanical property studies, and degradation in a solution of glutathione was complete after 5 h.

Finally, Palem et al. [150] prepared silver nanocomposite hydrogels via in situ addition of guar gum-*g*-poly(acrylamidoglycolic acid), silver nitrate, and sodium borohydride. The hydrogels were apparently self-healing owing to the dynamic covalent interactions between the borax and cis-diol groups, but also due to different interactions, such as intermolecular hydrogen bonding and strong hydration during the process. An MTT assay toward the CCD-986sk cell lines confirmed the cytocompatibility of the hydrogels.

7. Degradable hydrogels and elastomers with self-healing properties in biomedical applications

7.1. Self-Healable Hydrogels in Biomedical Applications

Self-healing hydrogels are attracting increasing interest in the biomedical field owing to their similarities to biological systems (**Table 11**). Among the self-healing hydrogels, injectable hydrogels are critical. These hydrogels may be extruded through a syringe as liquids due to their shear-thinning behaviors and

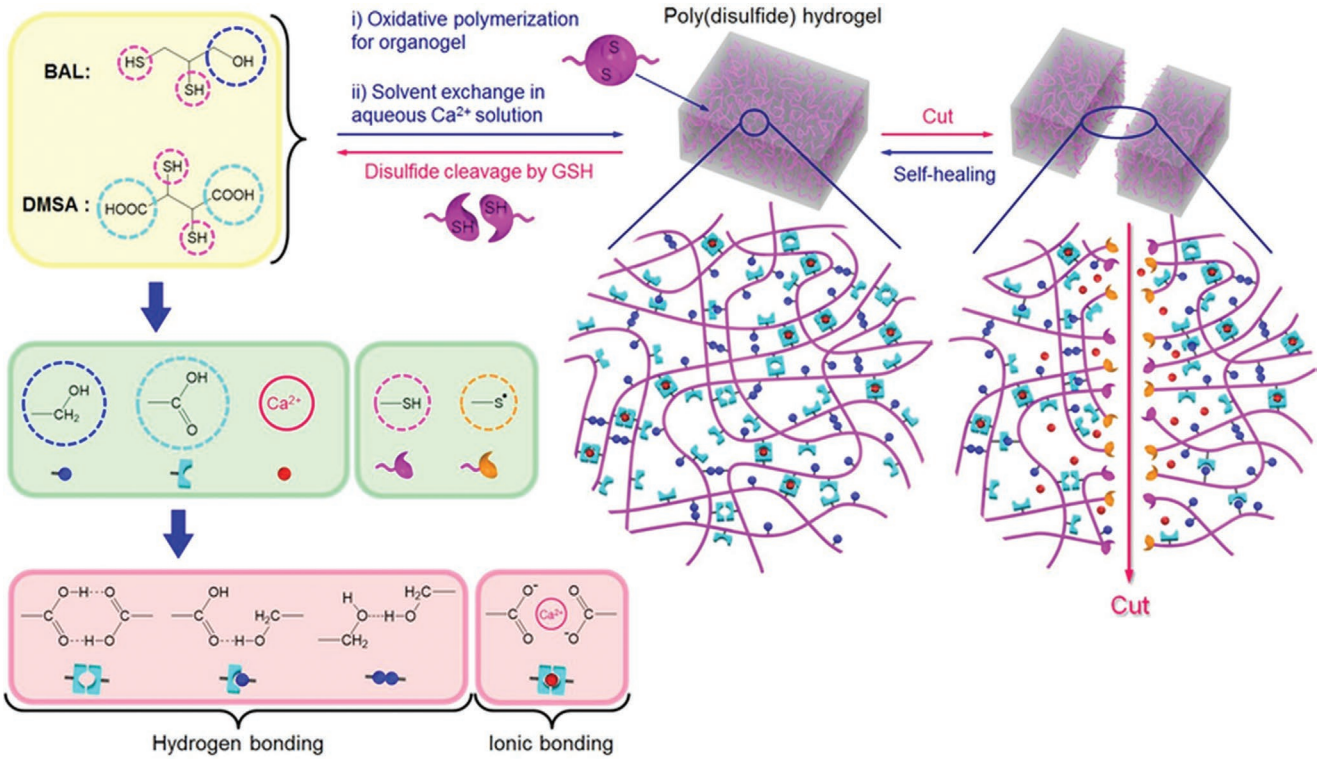

Figure 9. Schematic structure of degradable hydrogel based on 2,3-dimercapto-1-propanol and meso-2,3-dimercaptosuccinic acid copolymers – P(BAL-*co*-DMSA) – cross-linked with divalent ion Ca^{2+} and its self-healing mechanism. Adapted with permission.[149] Copyright 2020, Elsevier.

Table 11. Degradable self-healing hydrogels and elastomers and their potential applications in the biomedical field.

Mechanism	Nature	Materials	Potential biomedical applications	Ref.
Schiff base	Hydrogel	Phenol-functionalized chitosan/PEG-BA	3D Bioprinting	[40]
		Glycolated chitosan/PEG-BA	Tissue engineering, vascular repair	[42]
		Chitosan-g-aniline/PEG-BA	Cell delivery	[33]
		CMC/PEG-BA	Hemostasis	[43]
		Quaternized methacryloyl chitosan/PEG-BA	Wound healing	[44]
		Zwitterionic L-GA acid-functionalized chitosan/PEG-BA	Delivery	[45]
		CEC/PEG-BA/Polyacrylamide	Tissue engineering, actuators, wearable devices	[46]
		CEC/A-HA	Drug delivery for tumor therapy	[36]
		N-succinyl-chitosan/Chondroitin sulfate multiple aldehydes	Cell delivery and tissue engineering	[31]
		CEC/A-Alg	Cell delivery	[32]
		CMC/Aldehyde-functional carboxymethyl cellulose	Cell delivery	[37]
		Glycolated chitosan/A-Dex	Protein release	[35]
		CMC/A-Dex	Prevention and treatment of postoperative adhesion	[48]
		CEC/Dextran-g-aniline tetramer-g-4-formylbenzoic acid	Tissue engineering and cell delivery	[34]
		Acrylamide modified chitin/A-Alg	Drug delivery and tissue engineering	[38]
		CMC/A-Alg/Hap/CaCO3	Tissue engineering and drug delivery	[50]
		CMC/A-Alg/MGMs	Tissue engineering and drug delivery	[51]
		L-arginine conjugated chitosan/PEG-BA/pDA-NPs	Wound dressing	[54]
		CMC/Poly(dextran-g-4-formylbenzoic acid)/Peptide nanofibers	Wound healing	[55]
		Ethylenediamine functional gelatin/Dialdehyde carboxymethylcellulose	Drug and cell delivery and tissue engineering	[57]
		Aldehyde-modified xanthan gum/Phosphatidylethanolamine liposomes	Cell delivery and tissue engineering	[58]
Boronate ester bonds	Hydrogel	Poly(methacryloyloxyethyl phosphorylcholine) functionalized with benzoxaborole or catechol pendant groups	Drug delivery and tissue engineering	[61]
		5-methacrylamido-1,2-benzoxaborole/3-gluconamidoprpyl methacrylamide/Acrylamide	Bioprinting and cell encapsulation and delivery	[62]
		Nopoldiol/2-glucoamidoethylmethacrylamide/PEG methyl ether methacrylate/MAABO	Gene delivery, cell therapy, and tissue engineering	[63]
		Poly(DMA-st-MAABO)/2-lactobionamidoethyl methacrylamide, exhibiting galactose residues on the surface	Tissue engineering and drug delivery	[64]
		Dopamine functionalized 4-armed PEG/Phenylboronic acid modified 4-armed PEG	Bioadhesion, drug delivery, and tissue engineering	[65]
		PVA/Poly(aspartic acid) derivatives with boronic acid groups	Wound dressing, tissue repairing	[66]
		PVA/Carboxyethyl cellulose grafted with phenylboronic acid	Tissue engineering, wound healing, and drug delivery	[68]
		Methacrylated hyaluronic acid/3-aminophenylboronic acid-modified sodium alginate	Cell delivery and tissue regeneration	[69]
		PVA/Poly(acrylamide-*co*-dopamine methacrylamide) bis(phenylboronic acid carbamoyl) cystamine	Drug delivery in cancer treatment	[70]
		CTL/Boric acid/Mannitol	Tissue engineering cartilage regeneration	[71]
Hydrazone bonds	Hydrogel	Tetraphenylethylene-poly(DMA-stat-diacetone acrylamide)2/Acylhydrazide functionalized pectin	Drug delivery and tissue engineering	[72]
		Pectin aldehyde/Poly(NIPAM-stat-acylhydrazide)	Anticancer drug carrier	[73]
		A-HA/Hydrazide-HA	RNA delivery	[74]
		Adipic dihydrazide-grafted carboxyethyl chitin/PEG-BA Phe-NH2	Drug and cell delivery for tissue regenerative medicine	[75]
		Oxidized xanthan/8-arm PEG-hydrazine	Chemotherapeutic agent delivery, cell therapy, and tissue engineering	[76]
		Multi-hydrazide PEG/A-HA/Gelatin	Improving cell engraftment and retention	[77]
		Pectin achlydrazide/Poly(DMA-stat-4-FPA)	Tissue engineering, drug delivery, and biosensors	[78]

Table 11. Continued.

Mechanism	Nature	Materials	Potential biomedical applications	Ref.
		A-HA/3,3′-dithiobis(propionic hydrazide)	Tissue adhesive	[79]
		P(NIPAM-FPA-DMA)/3,3′-dithiobis (propionohydrazide) PEO dihydrazide	Drug delivery, tissue engineering, cell culture	[6]
		PAEH/Dialdehyde-PEG	Tissue repairing and drug release	[80]
Disulfide bonds	Hydrogel	BSA	Tissue engineering and 3D bioprinting	[81]
Hydrogen bonds	Hydrogel	Cytosine and guanosine-modified HA/1,6-hexamethylenediamine	Drug delivery, tissue engineering, cell scaffold materials, and regenerative medicine	[91]
		BSA/Epychlorhydrin	Drug delivery	[92]
	Elastomer	PGS with UPy	Tissue engineering and drug delivery	[98]
		PSeD with UPy	Tissue engineering	[99]
Hydrophobic interactions	Hydrogel	Ferrocene-modified chitosan	Drug delivery	[102]
		Alginate/Micelles of regenerated silk fibroin incorporating stearyl methacrylate	Drug delivery and tissue engineering	[103]
		4-arm poly(ethylene glycol)-b-poly(γ-o-nitrobenzyl-L-glutamate)	Drug delivery	[101]
Host-guest interactions	Hydrogel	HA-Ad/HA-CD	Drug and cell delivery	[104]
		β-cyclodextrin-modified PGA/Cholesterol-modified triblock PGA-b-PEG-b-PGA	Tissue engineering and drug delivery	[106]
		β-CD-modified alginate/Adamantine-modified graphene oxide	Tissue engineering	[105]
		Poly(CD) Acrylamide/*N*-vinyl-pyrrolidinone	Drug delivery	[107]
Electrostatic/Ionic interactions	Hydrogel	Chitosan/Carboxymethyl cellulose	Drug delivery	[108]
	Elastomer	PCL diol modified with IPDI before chain extension with anionic oligo-alginate and cationic *N*-methyldiethanolamine	Tissue engineering	[109]
Metal-coordination	Hydrogel	CMC/EDTA:Fe^{3+}/Silver nanoparticles	Wound healing	[112]
		CMC/(Fe^{3+}/Al^{3+})	Tissue engineering	[113]
		CMC/PCAD/Al^{3+}	Tissue sealant	[114]
		Polyaspartamide/histamine conjugate with/Cu2+	Adhesive	[115]
		Thiolated BSA/Silver nitrate	Tissue engineering	[116]
Combination of dynamic chemical bonds	Hydrogel	Gelatin/A-Alg/Adipic acid dihydrazide	Tissue engineering and drug delivery	[118]
		Gelatin/A-Dex/Adipic acid dihydrazide/bFGF@PLGA/Chlorhexidine acetate	Drug delivery and wound healing	[119]
Combination of physical interactions	Hydrogel	Polyglycerol sebacate/PEG methyl ether methacrylate/α-CD	Drug delivery	[124]
		Denatured BSA	Drug delivery	[125]
		Gelatin methacrylate/2-(2-methoxyethoxy)ethyl methacrylate	Cell culture, cell delivery, and tissue engineering	[126]
		Gelatin/PEDOT:PSS/MWCNTs-COOH	Wound healing	[127]
		Poly(glycerol sebacate)-co-poly(ethylene glycol)-g-catechol/Fe^{3}+/UPy-functional gelatin	Wound healing and wound closure	[132]
		κ-carrageenan/PAA/Zr^{4+}/D-galactose/Micelles of n-octadecyl acrylate dissolved in sodium dodecyl sulfate	Tissue engineering	[134]
	Elastomer	Polyurethane (PCL/HDI)/Sulfated alginate	Tissue engineering	[130]
Combination of dynamic chemical bonds and physical interactions	Hydrogel	Quaternized chitosan/Benzaldehyde-terminated Pluronic micelles	Wound healing	[136]
			Wound dressing	[137]

Table 11. Continued.

Mechanism	Nature	Materials	Potential biomedical applications	Ref.
		Catechol modified poly(L-lysine)/A-Dex/Fe	Wound healing	[138]
		Catechol-modified oxidized HA/Aminated gelatin/Fe^{3}+	Wound dressing	[139]
		Chitosan/Vanillin	Tissue engineering and wound repairing	[141]
		Poly(DMA-st-META-st-LAEMA)/Poly (MPC-st-UPyHEMA-st-MABBO)	Cell and tissue engineering	[143]
		Furfural-pectin/6-maleidocaproic acid chitosan	Drug delivery	[145]
		PVA/Borax/Cellulose nanofibers/Dopamine-grafted oxidized carbomethyl cellulose	Wound healing	[147]
		BOC/Gelatin/BOC-doped polypyrrole	Treatment of traumatic spinal cord injury	[148]
		Guar gum-g-poly(acrylamidoglycolic acid)/Silver nitrate/Sodium borohydride	Wound healing	[150]

A-Alg, aldehyde modified alginate; A-Dex, aldehyde modified dextran; A-HA, aldehyde modified hyaluronic acid; Ad, adamantane; bFGF@PLGA, PLGA microspheres integrated with basic fibroblast growth factor; BOC, borax-functionalized oxidized chondroitin sulfate; BSA, bovine serum albumin; CD, cyclodetrin; CEC, carboxyethyl chitosan; CMC, carboxymethyl chitosan; CTL, lactose modified chitosan; DMA, *N-N*-dimethylacrylamide; FPA, formylphenyl acrylate; HA, hyaluronic acid; HAp, hydroxyapatite; HDI, hexamethylene diisocyanate; IPDI, isophorone diisocyanate; MAABO, 5-methacrylamido-1,2-benzoxaborole; MGMs, magnetic gelatin microspheres; MWCNTs, multi-walled carbon nanotubes; NIPAM, N-isopropylacrylamide; PAA, poly(acrylic acid); PAEH, poly(aspartic acid) derivatives with hydrazide functional groups; PCAD, photoluminescent citric acid derivatives; PCL, polycaprolactone; pDa-NPs, polydopamine nanoparticles; PEG, poly(ethylene glycol), PEG-BA, benzaldehyde-poly(ethylene glycol); PEO, poly(ethylene oxide); PGS, poly(glycerol-*co*-sebacate); PSeD, poly(sebacoyl diglyceride); PVA, poly(vinyl alcohol); UPy, 2-ureido-4[1H]-pyrimidinone.

then reform into solid gels in situ. In most studies discussed in this review, these hydrogels are presented as potential candidates for use in biomedical applications, such as drug delivery, encapsulation of cells or proteins, tissue engineering, and wound dressing (**Figure 10**). However, these assertions have not been demonstrated and are only described as perspectives. In this section, we focus on the systems discussed in this review, for which proofs of concept for specific medical uses were clearly reported.

7.1.1. Self-Healable Hydrogels for Use in Wound Dressing

Numerous self-healing hydrogels have been applied in wound healing.[44,48,54,55,66,69,113,119,127,132,136–138,147,150] The skin acts as a protective barrier, and rapidly repairing skin damage that may be caused by trauma or burns or various diseases is crucial. Numerous hydrogels exhibit antibacterial properties, e.g., Ling et al. produced a self-healing hydrogel with antibacterial and angiogenic activities to accelerate skin wound healing.[54] The addition of pDA-NPs to chitosan/PEG-BA gels improved the inhibition of bacterial growth and enhanced angiogenesis. When evaluated in a rat model, wound healing was accelerated compared to that in the control group (99% versus 79%). In another example, Shen et al. reported that their poly(aspartic acid)-based system exhibited accelerated wound repair and improved skin cell proliferation owing to the prevention of bacterial infections in mice in vivo.[66] Hydrogels composed of *N,O*-CMC and A-Dex were fabricated as wound dressings and for use in preventing and treating postoperative adhesions.[48] The occurrence of postoperative adhesions in rat models with damaged sidewalls was significantly reduced (10%) in vivo, and furthermore, these gels could prevent infection and reduce inflammation. Qiu et al. developed chitosan-based hydrogels containing peptide nanofibers to heal chronic wounds.[55] This system exhibited antibacterial and hemostatic properties, which enabled the elimination of bacterial biofilms and induced blood-cell and platelet aggregation. Antibacterial adhesive injectable hydrogels were also designed as wound dressings for use in joint skin wound healing,[136] and the quaternized chitosan/benzaldehyde-terminated Pluronic system was evaluated in vivo. Accelerated wound healing due to curcumin-loaded hydrogels was revealed by higher granulation tissue thickness, collagen deposition, and upregulated vascular endothelial growth factor. Wang et al. developed a self-healing antibacterial hydrogel composed of quaternized methacryloyl chitosan and PEG-BA for use in wound treatment.[44] The gel displayed anti-infection properties and promoted the healing of infected wounds in vivo. Antimicrobial hydrogels reinforced with cellulose were

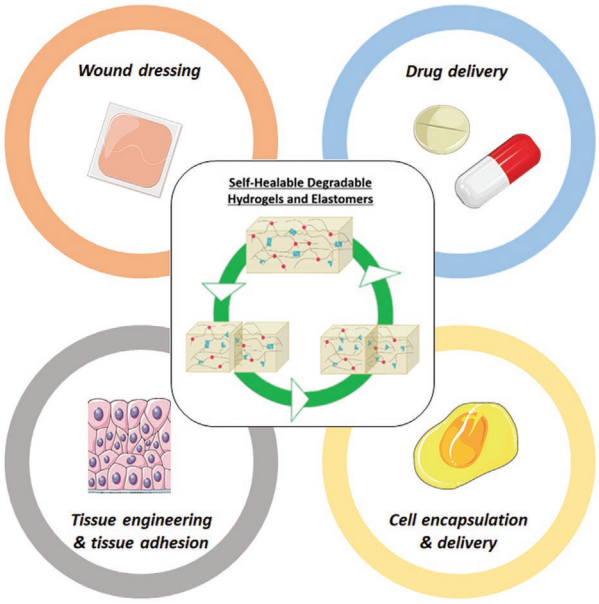

Figure 10. Potential biomedical applications of degradable self-healing hydrogels and elastomers.

prepared using PVA and borax.[147] They were impregnated with neomycin and appeared to be effective against numerous bacteria occurring in wounds. Chen et al. produced self-healing hydrogels for use in the sequential delivery of growth factors and antibacterial agents to heal wounds.[119] The gels were composed of aminated gelatin, adipic acid dihydrazide, and oxidized dextran and embedded with bFGF@PLGA microspheres and CHA. In vivo studies of the wounded skins of rats confirmed that the gels could prevent infection due to the delivery of CHA. Moreover, cell proliferation and wound healing could be accelerated via the release of bFGF. Another study reported conductive adhesive hydrogel wound dressings for use in the photothermal therapy of infected skin wounds.[137] The hydrogels were based on chitosan, benzaldehyde-terminated Pluronic, and CNTs and exhibited photothermal antibacterial properties in vivo. They could significantly improve wound healing, collagen deposition, and angiogenesis. To continue with photothermal antibacterial activity, Guo et al. developed self-healing hydrogel adhesives for use in wound closure or healing.[132] In vivo studies revealed that these gels could effectively kill methicillin-resistant *S. aureus*, exhibited good hemostatic properties, and enabled superior wound closure and healing of skin incisions compared to that observed using medical glue or surgical sutures. Self-healable, electroactive hydrogels based on gelatin were designed by Zheng et al. for use in motion sensing and acceleration of skin wound recovery via electrical stimulation.[127] An in vivo study performed using a full-thickness rat skin defect model highlighted a faster wound recovery with wound area reduction, granulation tissue formation, collagen deposition improvement, vascularization, and re-epithelialization. Finally, Palem et al. reported guar gum-grafted-poly(acrylamidoglycolic acid)-based hydrogels containing nano-silver, which appeared to accelerate wound healing.[150]

7.1.2. Self-Healable Hydrogels for Use in Drug Delivery

Drug delivery also benefits from the design of self-healing hydrogels.[36,50,51,73,74,76,78,80,92,100,101,108,118,124] Several methods may be used to control drug release, and two systems that involve magnetic fields have been reported. A self-healing chitosan-alginate hydrogel incorporating MGMs was designed for use in drug delivery.[51] When the gels were exposed to an external magnetic field, the drug release exhibited no clear difference in the early stage but significantly increased after the fifth day to reach 75% (compared to 60% without a magnetic field). In the second example, hydrogels were prepared using chitosan and cellulose and impregnated with magnetic chitosan microspheres.[108] Under an external magnetic field, the release increased to 91% compared to 62% without stimulation.

Self-healing hydrogels have been studied for use in anticancer treatment, and drug release is often controlled by pH. Bilalis et al. used a polypeptide system that could release gemcitabine to treat pancreatic cancer.[100] The injectable hydrogel was responsive to pH, and thus, only melted close to the pancreatic cancer cells, which enabled a targeted release of the drug toward cancerous tissues. An injectable BSA hydrogel was developed by Upadhyay et al. for use in controlled drug release toward cancer cells.[92] Once loaded with doxorubicin (Dox), the hydrogels could kill 70–80% of cancer cells. Sharma et al. prepared xanthan-PEG hydrogels loaded with Dox that exhibited pH-responsive drug release.[76] Drug delivery was accelerated at tumoral pH compared to that at physiological pH. Polysaccharide-based hydrogels designed by Qian et al. also demonstrated pH-responsive Dox release in PBS at various pH values.[36] Dox was released more rapidly under acidic conditions than in an alkaline medium, and the drug-loaded gels induced the deaths of HeLa cancer cells. In another example, pectin aldehyde was used in combination with an acylhydrazide-functionalized polymer to prepare an injectable system with anticancer drug-releasing properties.[73] Gels loaded with Dox and combretastatin A4 disodium phosphate affected CT26 tumors in vivo. Zhao et al. reported photodegradable self-healing hydrogels composed of PEG and polypeptides.[101] This system exhibited Dox release under UV irradiation due to the presence of photolabile *o*-nitrobenzyl ester groups. Increasing the amount of Dox released improved the apoptosis ratio of the HeLa cells. Another example of a Dox-loaded hydrogel is a poly(glycerol sebacate)-based system, which was reported as an injectable matrix.[124] Dox release was studied in vitro and exhibited a biphasic profile. The first phase was driven by diffusion, whereas the second phase was driven by hydrogel erosion.

The last two systems were designed to release proteins or small interfering ribonucleic acids (siRNAs). Cho et al. reported an injectable system prepared using glycol chitosan and A-Dex, and revealed that the release kinetics of BSA could be tuned by adjusting the needle size upon injection.[35] This could be explained by the modulation of the sizes and shapes of the fragmented hydrogels after passing through the needles. Wang et al. designed hydrogels for use in siRNA sequestration and initiated delivery to the heart.[74] Their system released siRNA on demand in response to proteolytic activity after myocardial infarction.

7.1.3. Self-Healable Hydrogels for Use in Cell Encapsulation and Delivery

Various self-healable hydrogels have been used in cell encapsulation and delivery,[31–33,58,61,69,75–77,126,135] e.g., a self-healing conductive injectable hydrogel based on chitosan and PEG-BA was prepared as a cell-delivery carrier for use in cardiac cell therapy.[33] The conductivities of the hydrogels were similar to that of native cardiac tissue. C2C12 myoblasts proliferated in the gels, and their viabilities were maintained after injection. Moreover, C2C12 myoblasts and H9c2 cardiac cells could be released at tunable rates. Yang et al. studied chitin hydrogels that could support the proliferation and multipotent differentiation of rat bone marrow-derived stem cells, and these hydrogels could be used as 3D scaffolds in stem-cell encapsulation and release.[75] Ma et al. developed an injectable polymer-liposome hydrogel as a cell carrier, wherein encapsulated cells were viable for an extended duration.[58] Several systems for use in cell retention have also been identified. Recently, stem cell transplantation emerged as a promising method of treating numerous diseases and injuries. However, although cell transplantation via injection is the preferred method of targeted cell delivery, this therapy results in low cell retention and engraftment. Cai et al.

studied injectable hydrogels that could resolve the problem of cell death after transplantation.[135] Their system, which was composed of a peptide-PEG copolymer assembled with a recombinant protein and PNIPAM chains conjugated to PEG, could protect the cells from mechanically disruptive forces during needle injection and provide a suitable 3D microenvironment for cell survival and retention. Moreover, in another system, hydrogels could enhance the survival, attachment, and engraftment of cells due to rapid sol-gel transitions.[77] Another hydrogel was prepared by Ren et al. to modulate the retention of transplanted cells.[126] As in the previous example, stem cells delivered within the gel were well protected from mechanical damage, which led to improved cell retention for three weeks in vivo.

7.1.4. Self-Healable Hydrogels for Use in Tissue Engineering and Tissue Adhesion

Self-healing hydrogels may be useful in bone tissue engineering. An injectable polysaccharide hydrogel loaded with HAp and calcium carbonate was developed for use in the regeneration of irregular bone defects.[50] Liu et al. prepared a protein-based hydrogel that was injected into large cranial defects of rabbits as a scaffold with osteoinductive and osteoconductive activities.[116] These in vivo studies revealed improved and accelerated bone repair. Another system was designed to repair the central nervous system.[41] The growth of neurosphere-like progenitors was accelerated within the hydrogels, and they could differentiate into neuron-like cells. The injection of this hydrogel enabled an 81% recovery of neural development. Hsieh et al. designed a biodegradable self-healing chitosan-fibrin hydrogel to induce blood-capillary formation,[42] and vascular endothelial cells seeded in this hydrogel could form capillary-like structures. Luo et al. reported the development of an injectable, electroconductive hydrogel to enhance tissue repair after traumatic spinal cord injury by bridging cavity spaces.[148] The gels exhibited mechanical and conductive properties similar to those of natural spinal cord tissues and could promote neuronal differentiation, improve axon outgrowth, and inhibit astrocyte differentiation in vitro. Significant locomotor functions were restored in rats with spinal cord injuries in vivo.

Finally, the development of self-healing hydrogels as tissue adhesives remains in progress. Identifying an acceptable compromise between the adhesive strength, mechanical properties, and degradation rate is often challenging. Xu et al. fabricated an injectable, self-healing, multi-responsive hydrogel as an on-demand dissolution tissue adhesive.[79] The system based on A-HA and a disulfide-containing cross-linker was compared to the commercial tissue adhesive BioGlue and exhibited an increased lap shear strength on porcine skin (up to 120 kPa, which is 65.8% higher than that of BioGlue). Li et al. developed another bioadhesive hydrogel that could efficiently close an open wound and enable post-wound-closure care.[138] In this case, the gel was composed of catechol-modified poly(lysine) and oxidized dextran and it enabled post-closure care after efficiently closing the skin incisions, as the bioadhesive could be easily removed and reapplied to the reopened wounds.

7.2. Self-Healable Elastomers in Biomedical Applications

Although less common than hydrogels, degradable, biocompatible elastomers are useful in the field of biomedical engineering because they mimic the mechanical properties of numerous soft tissues while resisting multiple mechanical stresses (Table 11). They are accepted by host tissues and resorb over time, thus avoiding possible inflammation and complications. However, once the chemically cross-linked elastomer is damaged, it cannot be repaired and thus may lead to complications in the healing of the host tissue. Therefore, the development of self-healing elastomers is necessary for use in biomedical applications, particularly in complex, dynamic in vivo environments.

Wu et al. synthesized PGS and grafted a UPy unit onto PGS (PGS-U) via HDI groups.[98] They focused on the elaboration of multifunctional 3D materials to deliver drugs, yield an antibacterial surface, and enable a cellular tri-culture. For drug delivery, 5-aminosalicylic acid (5-ASA) was incorporated into a PGS-4U film (ratio of 4/10 between the UPy and PGS units). A sandwich material consisting of the superposition of two layers without embedded 5-ASA and one layer with 5-ASA displayed linear release for 18 d. In parallel, antibacterial poly-L-lysine-UPy was physically associated with the PGS-U films via hydrogen bonding using drop casting. The antibacterial activity of the modified PGS-U against Gram-negative *E. coli* was confirmed, with a bactericidal ratio of up to 100% and no observable colony-forming units. Finally, to reconstruct tissues at the interface between the ligament, cartilage, and bone, PGS-U was used as a co-culture system for L929 fibroblasts, chondrocytes, and MC3T3 osteoblasts. Cells were cultured on independent films before exploiting the self-healing properties of PGS-U in pressing these films together at 37 °C for 1 min to generate a single culture surface.

Daemi et al. used a natural polymer based on alginate with cationic PU to achieve a tensile strength of 10 MPa for vascular applications.[109] Cytocompatibility was confirmed in vitro using L929 fibroblasts and human umbilical vein endothelial cells, whereas a mild inflammatory response 20 d post-implantation was observed in vivo in rat tissues, with the formation of new vessels. In addition, the same group modified its initial cationic polymer to decrease its toughness (61 MJ m^{-3}).[130] With the highest amount of sulfated alginate, it displayed superior anticoagulation activity and blood compatibility and no cytotoxicity or chronic inflammation after in vivo implantation into Wistar rats for 8 weeks. In vivo degradation following subcutaneous implantation resulted in the remaining mass decreasing to 85% after 8 weeks.

The last example concerns tissue reconstruction (soft or hard). Jiang et al. designed self-healable elastomers based on PUs with dual-dynamic bonds (oxime-urethane and hydrogen bonds).[146] After demonstrating their viabilities, they were applied to 1) limit the progression of aortic aneurysms, 2) heal the sciatic nerve, and 3) immobilize the sternum (**Figure 11**). The assays were performed in vivo in mice using soft or hard elastomers, depending on the ratio of glycerol used in their preparation. First, to limit the progression of aortic aneurysms, arteries were wrapped with elastomers, and the optimal in vivo results were obtained using elastomers with E values similar to that of the vascular tissue (1 MPa). Second, in nerve reconstruction, a softer elastomer with a lower glycerol content

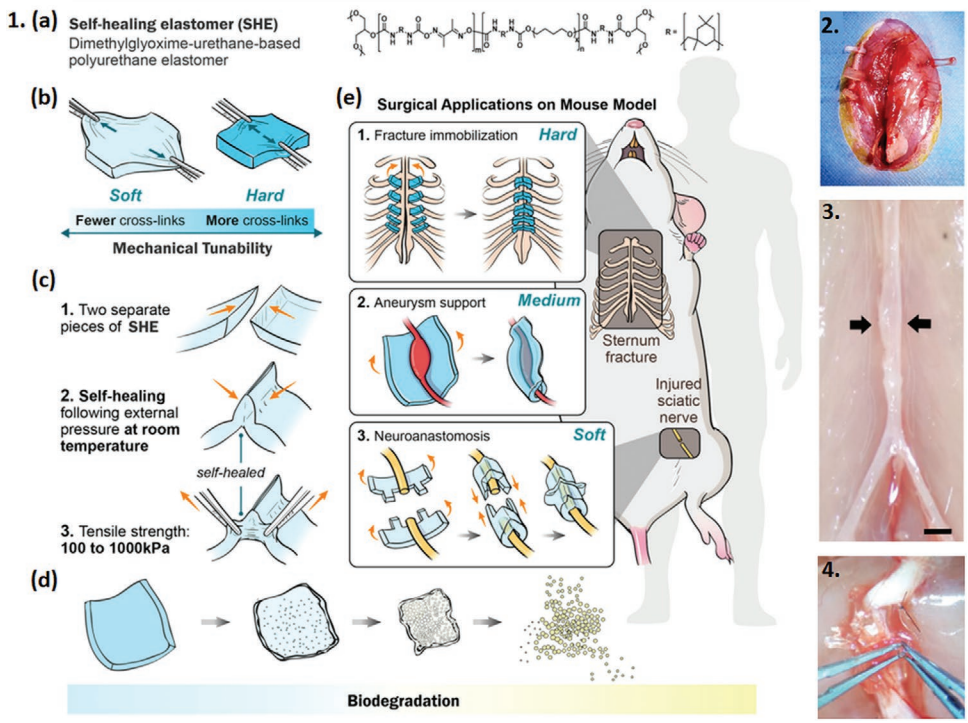

Figure 11. 1) Schematic diagram of chemical structure formula, tunable mechanical and self-healing properties, and in vivo biomedical applications. 2) Sternum immobilization by elastomer in rat. 3) Gross observations of aorta with cross-linked self-healing elastomer (SHE). The blood vessel pointed by the black arrow is the abdominal aorta, scale bar = 1 mm. 4. Paper-cut simulation (clip) of sciatic nerve coaptation. Adapted with permission.[146] Copyright 2021, Nature.

was used. A film of this elastomer was cut in half to yield ends with castle-like shapes, and each nerve end was wrapped in the film. Once the ends were joined, they displayed a weld that was three- to four-fold faster than sutures. This material exhibited superior repair results than those obtained using sutures, fibrin glue, and PCL conduit groups. Finally, a hard elastomer (with a high glycerol content) was used in bone repair after fracture. After 6 weeks, the fracture was repaired without a pneumothorax, and the results were identical to those obtained using the steel wire control.

8. Concluding Remarks, Opportunities, and Challenges

In this review, we analyzed the latest examples of self-healable degradable hydrogels and elastomers for use in biomedical applications, including tissue engineering, drug delivery, and wound repair. The nature of the dynamic cross-linking, covalent or physical, was described, in addition to the conditions/stimuli required to induce self-healing (e.g., heat and pH). We focused on the most recent degradable networks that combine at least two self-healing mechanisms, in particular. To provide a useful compilation for readers and aid them in selecting potential strategies for their requirements, we also analyzed the mechanical properties, repair time, and SHE. These properties are summarized in the diagrams shown in **Figure 12** and presented as functions of the natures of the self-healing mechanisms of the degradable networks analyzed. These diagrams confirm that most of the networks exhibit high SHEs of >75%, regardless of the type of self-healing. The time required to obtain a high SHE highlights the superiority of networks with multiple self-healing mechanisms. Their repair times, although similar to those observed with dynamic chemical bonds, are clearly superior to those of self-healing networks with only physical interactions, which display a wide range of repair times (Figure 12.1). Furthermore, a large range of mechanical properties, from a few pascals to a few tens of megapascals, may be realized using degradable self-healing networks based on physical interactions (Figure 12.2), as this class of biomaterials includes most elastomers listed in this review. In comparison, the networks with self-healing based on chemical bonds discussed in this review are mostly characterized by moduli of ≈ 10 kPa, whereas the moduli of the networks with dual self-healing mechanisms lie in between. Based on the systems analyzed here, a contradiction between mechanical strength and self-healing behavior is apparent. This may be due to the nature of the polymeric chains used in the various systems. Most self-healing systems are designed with hydrophilic polymers, which leads to a majority of self-healable hydrogels and a minority of self-healable elastomers. Consequently, most of the analyzed self-healing networks display poor mechanical properties. However, when considering only the elastomers, self-healing properties may also be imparted to stronger materials (e.g., $E >$ 150 MPa for systems based on PCL and DA reactions [86,87]).

As shown during this review, self-healable degradable/bioeliminable networks open large avenues in designing smart materials for use in biomedical applications and should

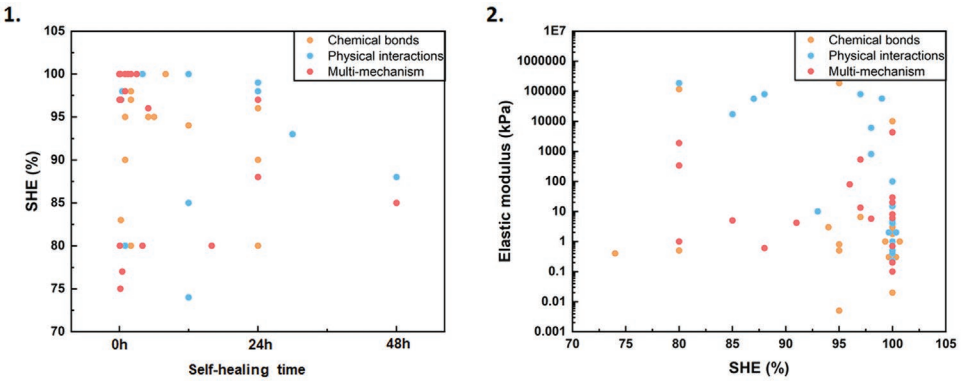

Figure 12. Compared properties of the self-healable degradable networks presented in the review as a function of the nature of the self-healing mechanism.

continue to attract attention due to their unique features, which may be summarized as follows (**Figure 13**). First, the range of mechanical properties that may be reached covers most of the requirements in soft-tissue engineering and repair, with moduli ranging from a few pascals for the softest hydrogels to a few tens of megapascals for elastomers. This opens opportunities to develop networks mimicking the extracellular matrix for use in cell culturing and delivery or engineer vessels, muscles, ligaments, etc., as only bones and their mechanical properties are currently out of reach for the reported materials. Second, the healing times may be as fast as a few seconds, depending on the reversible bonds and the mobility of the polymer chains. Clearly, this time also depends on the parameter that is retained to evaluate self-healing, as the time required for visual repair may be drastically shorter than the time required for the recovery of the mechanical properties. A third advantage with respect to their biomedical applications is their degradability, which may exhibit large variations in degradation time, from hours to months, depending on the individual components used: hydrophilic or hydrophobic chains, biopolymers or synthetic chains, and hydrolytic or enzymatic degradation. Finally, the intrinsic multifunctionality of these systems renders them particularly attractive for use in drug delivery because the interactions responsible for the dynamic network may be exploited to increase the loading and retention of drugs and biologics (e.g., ionic interactions and hydrogen bonding).

However, these clear opportunities should not conceal the challenges that remain (Figure 13). The first challenge is the design of stronger networks. As shown in this review, hydrogels reign supreme in the field, but still lack resistance to mechanical stress and do not cover the entire spectrum of soft tissue reconstruction. Self-healable degradable elastomers are thus natural candidates to address this limitation, but very few studies have been conducted to date, as most efforts in the field focus on bio-based, recyclable, reprocessable elastomers that are not intended for biomedical use. This is particularly true for vitrimers, which are permanent chemical networks with dynamic covalent bonds that enable the network to change its topology while maintaining a constant number of chemical bonds. Although self-healable by nature, and in several cases based on the same dynamic bonds (e.g., imines and boronic esters), vitrimers are still rarely designed for use in biomedical applications.[151] In addition, combining covalent bonds and dynamic/reversible chemical bonds or noncovalent interactions/physical bonds may be investigated to provide self-healable, strong, degradable networks. Although the replacement of covalent bonds with dynamic bonds in networks diminishes their inherent mechanical strengths,[152] a sound ratio between the two types of bonds should ensure the mechanical properties while guaranteeing a degree of self-healing. Another challenge is the generation of additional characteristics along with self-healing. Microbial resistance, conductivity, and anisotropic and adhesive properties are examples of the characteristics necessary for developing a novel generation of smart biomaterials. Although the examples analyzed in this review illustrate these aspects, they remain rare and require more complex formulations that may hinder their translation to products or the use of potentially toxic precursors, threatening their biocompatibility. Another challenge lies in the definition of self-healing networks. Although dynamic bonds are the key prerequisite in self-healing networks, several composite materials based on non-dynamic cross-linked networks and thermoplastic chains

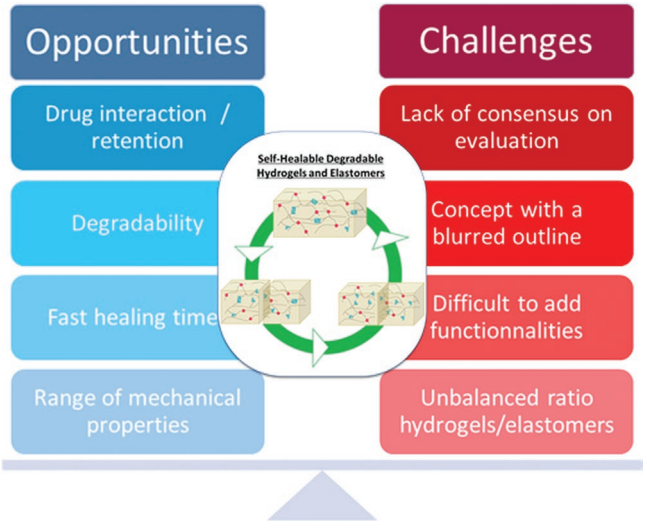

Figure 13. Summary of the opportunities and challenges associated with self-healable degradable networks for biomedical applications.

have been claimed as self-healable biomaterials. The use of free PCL chains that may flow at temperatures above their melting temperatures through the damaged network and promote the partial recovery of the mechanical and structural properties upon cooling is, for example, reported for degradable self-healable elastomers.[153] The extension of self-healing to hydrogels obtained via classical electrostatic or hydrophobic interactions is also questionable, as any shear-thinning hydrogel based on such mechanisms (e.g., alginate/Ca^{2+} gels or PLA-PEG-PLA triblock copolymer gels) could be considered as a self-healable biomaterial. Finally, the evaluation of self-healing properties is crucial in terms of two aspects. First, the self-healing capacities of the final devices or scaffolds are generally not evaluated. The possibility of processing 3D self-healable biomaterials has been investigated in previous studies using techniques such as 3D printing/bioprinting,[154] particle leaching,[155] freeze-drying,[156] thermally induced phase separation,[157] gas foaming,[158] solvent casting,[159] nanofiber self-assembly,[160] and fiber-based techniques.[161] However, the self-healing properties of 3D biomaterials have not been studied and should be investigated. Second, as shown in this review, various methods are used to estimate the repair time and SHE (Figure 3). Wide discrepancies remain in practice, rendering comparisons of the performances of materials challenging. This also renders the performance of any trend analysis, which is required for the future sound design of self-healable biomaterials dedicated to specific, demanding biomedical applications, challenging. More standardized methods (e.g., via a normative framework) to evaluate and quantify the self-healing properties to categorize self-healable materials are necessary to ensure further development and potential transfer to the market of this class of innovative biomaterials. In this sense, efforts to model the mechanics of self-healing polymer networks cross-linked via dynamic bonds may enable the more rational design of these systems. This may also enable comparison between them by offering tools to predict healing times and SHEs based on macromolecular and reactivity considerations.[27] Therefore, this aspect should be considered in optimizing self-healing degradable networks.

Acknowledgements

The authors thank the French Agency for Research (ANR) for support of LG through ANR2016-BIOSCAFF (ANR-16-CE09-0024) and of MG through ANR2019-OPENN (ANR-19-CE19-0022-02).

Conflict of Interest

The authors declare no conflict of interest.

Keywords

biomedical, degradable networks, elastomers, hydrogels, self-healing

Received: May 10, 2022
Revised: December 11, 2022
Published online: January 25, 2023

[1] S. Utrera-Barrios, R. Verdejo, M. A. López-Manchado, M. Hernández Santana, *Mater. Horiz.* **2020**, *7*, 2882.
[2] S. R. White, N. R. Sottos, P. H. Geubelle, J. S. Moore, M. R. Kessler, S. R. Sriram, E. N. Brown, S. Viswanathan, *Nature* **2001**, *409*, 794.
[3] M. Deng, F. Guo, D. Liao, Z. Hou, Y. Li, *Polym. Chem.* **2018**, *9*, 98.
[4] P. Wang, L. Yang, B. Dai, Z. Yang, S. Guo, G. Gao, L. Xu, M. Sun, K. Yao, J. Zhu, *Eur. Polym. J.* **2020**, *123*, 109382.
[5] S.-M. Kim, H. Jeon, S.-H. Shin, S.-A. Park, J. Jegal, S. Y. Hwang, D. X. Oh, J. Park, *Adv. Mater.* **2018**, *30*, 1705145.
[6] H. An, K. Xu, L. Chang, Y. Wang, J. Qin, W. Li, *Polymer* **2018**, *147*, 38.
[7] N. Kuhl, S. Bode, R. K. Bose, J. Vitz, A. Seifert, S. Hoeppener, S. J. Garcia, S. Spange, S. van der Zwaag, M. D. Hager, U. S. Schubert, *Adv. Funct. Mater.* **2015**, *25*, 3295.
[8] Y. Song, Y. Liu, T. Qi, G. L. Li, *Angew. Chem.* **2018**, *130*, 14034.
[9] A. J. R. Amaral, G. Pasparakis, *Polym. Chem.* **2017**, *8*, 6464.
[10] X. Wu, J. Li, G. Li, L. Ling, G. Zhang, R. Sun, C.-P. Wong, *J. Appl. Polym. Sci.* **2018**, *135*, 46532.
[11] Y. Peng, Y. Yang, Q. Wu, S. Wang, G. Huang, J. Wu, *Polymer* **2018**, *157*, 172.
[12] D. K. Smith, *Chem. Soc. Rev.* **2009**, *38*, 684.
[13] D. Ma, Y. Wang, W. Dai, *Mater. Sci. Eng. C* **2018**, *89*, 456.
[14] S. Doppalapudi, A. Jain, W. Khan, A. J. Domb, *Polym. Adv. Technol.* **2014**, *25*, 427.
[15] R. Muthuraj, M. Misra, A. K. Mohanty, *J. Appl. Polym. Sci.* **2018**, *135*, 45726.
[16] Medical Polymers Market Growth & Trends, https://www.grandviewresearch.com/press-release/global-medical-polymer-market, accessed: March, **2022**.
[17] Q. Chen, S. Liang, G. A. Thouas, *Prog. Polym. Sci.* **2013**, *38*, 584.
[18] C. Mangeon, E. Renard, F. Thevenieau, V. Langlois, *Mater. Sci. Eng. C* **2017**, *80*, 760.
[19] Y. Tu, N. Chen, C. Li, H. Liu, R. Zhu, S. Chen, Q. Xiao, J. Liu, S. Ramakrishna, L. He, *Acta Biomater.* **2019**, *90*, 1.
[20] N. Roy, B. Bruchmann, J.-M. Lehn, *Chem. Soc. Rev.* **2015**, *44*, 3786.
[21] L. Zhai, A. Narkar, K. Ahn, *Nano Today* **2020**, *30*, 100826.
[22] D. G. Bekas, K. Tsirka, D. Baltzis, A. S. Paipetis, *Compos. Part B Eng.* **2016**, *87*, 92.
[23] R. V. S. P. Sanka, B. Krishnakumar, Y. Leterrier, S. Pandey, S. Rana, V. Michaud, *Front. Mater* **2019**, *6*, 137.
[24] D. L. Taylor, M. in het Panhuis, *Adv. Mater.* **2016**, *28*, 9060.
[25] X. Yan, F. Wang, B. Zheng, F. Huang, *Chem. Soc. Rev.* **2012**, *41*, 6042.
[26] B. Cheng, X. Lu, J. Zhou, R. Qin, Y. Yang, *ACS Sustainable Chem. Eng.* **2019**, *7*, 4443.
[27] K. Yu, A. Xin, Q. Wang, *J Mech Phys Solids* **2018**, *121*, 409.
[28] S. Lyu, D. Untereker, *Int. J. Mol. Sci.* **2009**, *10*, 4033.
[29] E. Yousif, R. Haddad, *SpringerPlus* **2013**, *2*, 398.
[30] A. Banerjee, K. Chatterjee, G. Madras, *Mater. Sci. Technol.* **2014**, *30*, 567.
[31] S. Lü, C. Gao, X. Xu, X. Bai, H. Duan, N. Gao, C. Feng, Y. Xiong, M. Liu, *ACS Appl. Mater. Interfaces* **2015**, *7*, 13029.
[32] Z. Wei, J. Zhao, Y. M. Chen, P. Zhang, Q. Zhang, *Sci. Rep.* **2016**, *6*, 1.
[33] R. Dong, X. Zhao, B. Guo, P. X. Ma, *ACS Appl. Mater. Interfaces* **2016**, *8*, 17138.
[34] B. Guo, J. Qu, X. Zhao, M. Zhang, *Acta Biomater.* **2019**, *84*, 180.
[35] I. S. Cho, T. Ooya, *J. Biomater. Sci., Polym. Ed.* **2018**, *29*, 145.
[36] C. Qian, T. Zhang, J. Gravesande, C. Baysah, X. Song, J. Xing, *Int. J. Biol. Macromol.* **2019**, *123*, 140.
[37] J. Thomas, A. Sharma, V. Panwar, V. Chopra, D. Ghosh, *ACS Appl Bio Mater* **2019**, *2*, 2013.
[38] F. Ding, S. Wu, S. Wang, Y. Xiong, Y. Li, B. Li, H. Deng, Y. Du, L. Xiao, X. Shi, *Soft Matter* **2015**, *11*, 3971.
[39] S. Maity, A. Chatterjee, N. Chakraborty, J. Ganguly, *New J. Chem.* **2018**, *42*, 5946.
[40] Y. Liu, C. W. Wong, S. W. Chang, S. hui Hsu, *Acta Biomater.* **2021**, *122*, 211.

[41] T. C. Tseng, L. Tao, F. Y. Hsieh, Y. Wei, I. M. Chiu, S. H. Hsu, *Adv. Mater.* **2015**, *27*, 3518.
[42] F. Y. Hsieh, L. Tao, Y. Wei, S. H. Hsu, *NPG Asia Mater* **2017**, *9*, 1.
[43] W. Huang, Y. Wang, Y. Chen, Y. Zhao, Q. Zhang, X. Zheng, L. Chen, L. Zhang, *Adv. Healthcare Mater.* **2016**, *5*, 2813.
[44] L. Wang, K. Yang, X. Li, X. Zhang, D. Zhang, L. N. Wang, C. S. Lee, *Acta Biomater.* **2021**, *124*, 139.
[45] M. Khan, J. T. Koivisto, T. I. Hukka, M. Hokka, M. Kellomäki, *ACS Appl. Mater. Interfaces* **2018**, *10*, 11950.
[46] B. Fu, B. Cheng, X. Jin, X. Bao, Z. Wang, Q. Hu, *J. Appl. Polym. Sci.* **2019**, *136*, 1.
[47] S. H. Lin, C. M. Papadakis, J. J. Kang, J. M. Lin, S. H. Hsu, *Chem. Mater.* **2021**, *33*, 3945.
[48] H. Li, X. Wei, X. Yi, S. Tang, J. He, Y. Huang, F. Cheng, *Mater. Sci. Eng. C* **2021**, *123*, 111978.
[49] S. Li, J. Yi, X. Yu, H. Shi, J. Zhu, L. Wang, *ACS Biomater. Sci. Eng.* **2018**, *4*, 872.
[50] B. Ren, X. Chen, S. Du, Y. Ma, H. Chen, G. Yuan, J. Li, D. Xiong, H. Tan, Z. Ling, Y. Chen, X. Hu, X. Niu, *Int. J. Biol. Macromol.* **2018**, *118*, 1257.
[51] X. Chen, M. Fan, H. Tan, B. Ren, G. Yuan, Y. Jia, J. Li, D. Xiong, X. Xing, X. Niu, X. Hu, *Mater. Sci. Eng. C* **2019**, *101*, 619.
[52] Y. Zhang, B. Yang, X. Zhang, L. Xu, L. Tao, S. Li, Y. Wei, *Chem. Commun.* **2012**, *48*, 9305.
[53] S. Nardecchia, A. Jiménez, J. R. Morillas, J. de Vicente, *Polymer* **2021**, *218*, 123489.
[54] Z. Ling, Z. Chen, J. Deng, Y. Wang, B. Yuan, X. Yang, H. Lin, J. Cao, X. Zhu, X. Zhang, *Chem. Eng. J.* **2021**, *420*, 130302.
[55] W. Qiu, H. Han, M. Li, N. Li, Q. Wang, X. Qin, X. Wang, J. Yu, Y. Zhou, Y. Li, F. Li, D. Wu, *J. Colloid Interface Sci.* **2021**, *596*, 312.
[56] T. W. Lin, S. hui Hsu, *Adv. Sci.* **2020**, *7*, 1901388.
[57] J. Lei, X. Li, S. Wang, L. Yuan, L. Ge, D. Li, C. Mu, *ACS Appl Polym Mater* **2019**, *1*, 1350.
[58] Y. H. Ma, J. Yang, B. Li, Y. W. Jiang, X. Lu, Z. Chen, *Polym. Chem.* **2016**, *7*, 2037.
[59] W. Wang, L. Xiang, L. Gong, W. Hu, W. Huang, Y. Chen, A. B. Asha, S. Srinivas, L. Chen, R. Narain, H. Zeng, *Chem. Mater.* **2019**, *31*, 2366.
[60] H. Li, J. Bai, Z. Shi, J. Yin, *Polymer* **2016**, *85*, 106.
[61] Y. Chen, D. Diaz-Dussan, D. Wu, W. Wang, Y. Y. Peng, A. B. Asha, D. G. Hall, K. Ishihara, R. Narain, *ACS Macro Lett.* **2018**, *7*, 904.
[62] Y. Wang, L. Li, Y. Kotsuchibashi, S. Vshyvenko, Y. Liu, D. Hall, H. Zeng, R. Narain, *ACS Biomater. Sci. Eng.* **2016**, *2*, 2315.
[63] D. Wu, W. Wang, D. Diaz-Dussan, Y. Y. Peng, Y. Chen, R. Narain, D. G. Hall, *Chem. Mater.* **2019**, *11*, 4092.
[64] Y. Chen, W. Wang, D. Wu, H. Zeng, D. G. Hall, R. Narain, *ACS Appl. Mater. Interfaces* **2019**, *11*, 44742.
[65] M. Shan, C. Gong, B. Li, G. Wu, *Polym. Chem.* **2017**, *8*, 2997.
[66] J. Shen, Z. Zhou, D. Chen, Y. Wang, Y. He, D. Wang, J. Qin, *Colloids Surf B Biointerfaces* **2021**, *200*, 111568.
[67] H. Meng, P. Xiao, J. Gu, X. Wen, J. Xu, C. Zhao, J. Zhang, T. Chen, *Chem. Commun.* **2014**, *50*, 12277.
[68] H. An, Y. Bo, D. Chen, Y. Wang, H. Wang, Y. He, J. Qin, *RSC Adv.* **2020**, *10*, 11300.
[69] X. Zhang, Y. Li, D. He, Z. Ma, K. Liu, K. Xue, H. Li, *Chem. Eng. J.* **2021**, *425*, 130677.
[70] R. Guo, Q. Su, J. J. Zhang, A. Dong, C. Lin, J. J. Zhang, *Biomacromolecules* **2017**, *18*, 1356.
[71] F. Furlani, P. Sacco, M. Cok, G. De Marzo, E. Marsich, S. Paoletti, I. Donati, *ACS Biomater. Sci. Eng.* **2019**, *5*, 5539.
[72] H. An, L. Chang, J. Shen, S. Zhao, M. Zhao, X. Wang, J. Qin, *J. Polym. Res.* **2019**, *26*, 26.
[73] H. An, Y. Yang, Z. Zhou, Y. Bo, Y. Wang, Y. He, D. Wang, J. Qin, *Acta Biomater.* **2021**, *131*, 149.
[74] L. L. Wang, J. J. Chung, E. C. Li, S. Uman, P. Atluri, J. A. Burdick, *J. Controlled Release* **2018**, *285*, 152.
[75] X. Yang, H. Yang, X. Jiang, B. Yang, K. Zhu, N. Chun-Him Lai, C. Huang, C. Chang, L. Bian, L. Zhang, *Carbohydr. Polym.* **2020**, *256*, 117574.
[76] P. K. Sharma, S. Taneja, Y. Singh, *ACS Appl. Mater. Interfaces* **2018**, *10*, 30936.
[77] Y. Cai, M. Johnson, A. Sigen, Q. Xu, H. Tai, W. Wang, *Macromol. Biosci.* **2021**, *21*, 2100079.
[78] D. Chen, L. Chang, Z. Zhou, Y. Bo, Y. Wang, Y. He, J. Qin, *J. Polym. Res.* **2021**, *28*, 3.
[79] S. A, Q. Xu, M. Johnson, J. Creagh-Flynn, M. Venet, D. Zhou, I. Lara-Sáez, H. Tai, W. Wang, *Appl. Mater. Today* **2021**, *22*, 100967.
[80] H. An, L. Zhu, J. Shen, W. Li, Y. Wang, J. Qin, *Colloids Surf B Biointerfaces* **2020**, *185*, 110601.
[81] X. Zhang, S. Jiang, T. Yan, X. Fan, F. Li, X. Yang, B. Ren, J. Xu, J. Liu, *Soft Matter* **2019**, *15*, 7583.
[82] S. S. Rahman, M. Arshad, A. Qureshi, A. Ullah, *ACS Appl. Mater. Interfaces* **2020**, *12*, 51927.
[83] W.-Q. Yuan, G.-L. Liu, C. Huang, Y.-D. Li, J.-B. Zeng, *Macromolecules* **2020**, *53*, 9847.
[84] F. Li, Z. Xu, H. Hu, Z. Kong, C. Chen, Y. Tian, W. Zhang, W. Bin Ying, R. Zhang, J. Zhu, *Chem. Eng. J.* **2021**, *410*, 128363.
[85] X. Chen, *Science* **2002**, *295*, 1698.
[86] K. Inoue, M. Yamashiro, M. Iji, *J. Appl. Polym. Sci.* **2009**, *112*, 876.
[87] T. Defize, R. Riva, J.-M. Thomassin, C. Jérôme, M. Alexandre, *Macromol. Symp.* **2011**, *309–310*, 154.
[88] T. Defize, J.-M. Thomassin, M. Alexandre, B. Gilbert, R. Riva, C. Jérôme, *Polymer* **2016**, *84*, 234.
[89] L.-T. T. Nguyen, T. T. Truong, H. T. Nguyen, L. Le, V. Q. Nguyen, T. Van Le, A. T. Luu, *Polym. Chem.* **2015**, *6*, 3143.
[90] G. Rivero, L.-T. T. Nguyen, X. K. D. Hillewaere, F. E. Du Prez, *Macromolecules* **2014**, *47*, 2010.
[91] X. Ye, X. Li, Y. Shen, G. Chang, J. Yang, Z. Gu, *Polymer* **2017**, *108*, 348.
[92] A. Upadhyay, R. Kandi, C. P. Rao, *ACS Sustainable Chem. Eng.* **2018**, *6*, 3321.
[93] R. Chang, Y. Huang, G. Shan, Y. Bao, X. Yun, T. Dong, P. Pan, *Polym. Chem.* **2015**, *6*, 5899.
[94] W. Ren, Z. Li, Y. Chen, H. Gao, W. Yang, Y. Wang, Y. Luo, *Macromol. Mater. Eng.* **2019**, *304*, 1800491.
[95] D. Wan, Q. Jiang, Y. Song, J. Pan, T. Qi, G. L. Li, *ACS Appl Polym Mater* **2020**, *2*, 879.
[96] M. Wei, M. Zhan, D. Yu, H. Xie, M. He, K. Yang, Y. Wang, *ACS Appl. Mater. Interfaces* **2015**, *7*, 2585.
[97] M. Invernizzi, S. Turri, M. Levi, R. Suriano, *Eur. Polym. J.* **2018**, *101*, 169.
[98] Y. Wu, L. Wang, X. Zhao, S. Hou, B. Guo, P. X. Ma, *Biomaterials* **2016**, *104*, 18.
[99] S. Chen, X. Bi, L. Sun, J. Gao, P. Huang, X. Fan, Z. You, Y. Wang, *ACS Appl. Mater. Interfaces* **2016**, *8*, 20591.
[100] P. Bilalis, D. Skoulas, A. Karatzas, J. Marakis, A. Stamogiannos, C. Tsimblouli, E. Sereti, E. Stratikos, K. Dimas, D. Vlassopoulos, H. Iatrou, *Biomacromolecules* **2018**, *19*, 3840.
[101] D. Zhao, Q. Tang, Q. Zhou, K. Peng, H. Yang, X. Zhang, *Soft Matter* **2018**, *14*, 7420.
[102] Y. K. Li, C. G. Guo, L. Wang, Y. Xu, C. Y. Liu, C. Q. Wang, *RSC Adv.* **2014**, *4*, 55133.
[103] L. Meng, C. Shao, C. Cui, F. Xu, J. Lei, J. Yang, *ACS Appl. Mater. Interfaces* **2020**, *12*, 1628.
[104] C. B. Rodell, R. J. Wade, B. P. Purcell, N. N. Dusaj, J. A. Burdick, *ACS Biomater. Sci. Eng.* **2015**, *1*, 277.
[105] S. Soltani, R. Emadi, S. H. Javanmard, M. Kharaziha, A. Rahmati, *Int. J. Biol. Macromol.* **2021**, *180*, 311.
[106] G. Li, J. Wu, B. Wang, S. Yan, K. Zhang, J. Ding, J. Yin, *Biomacromolecules* **2015**, *16*, 3508.
[107] C. Yu, D. Alkekhia, A. Shukla, *ACS Appl Polym Mater* **2020**, *2*, 55.

[108] Z. Wang, X. Zhai, M. Fan, H. Tan, Y. Chen, *Eur. Polym. J.* **2021**, *157*, 110644.
[109] H. Daemi, S. Rajabi-Zeleti, H. Sardon, M. Barikani, A. Khademhosseini, H. Baharvand, *Biomaterials* **2016**, *84*, 54.
[110] M. Ginting, S. P. Pasaribu, I. Masmur, J. Kaban, Hestina, *RSC Adv.* **2020**, *10*, 5050.
[111] X. H. Wang, F. Song, D. Qian, Y. D. He, W. C. Nie, X. L. Wang, Y. Z. Wang, *Chem. Eng. J.* **2018**, *349*, 588.
[112] M. Pandian, V. Selvaprithviraj, A. Pradeep, J. Rangasamy, *Int. J. Biol. Macromol.* **2021**, *188*, 501.
[113] J. Cao, P. Wu, Q. Cheng, C. He, Y. Chen, J. Zhou, *ACS Appl. Mater. Interfaces* **2021**, *13*, 24095.
[114] Y. M. Chen, L. Sun, S. A. Yang, L. Shi, W. J. Zheng, Z. Wei, C. Hu, *Eur. Polym. J.* **2017**, *94*, 501.
[115] J. R. Moon, Y. S. Jeon, Y. J. Kim, J.-H. Kim, *J. Polym. Res.* **2019**, *26*, 12.
[116] W. Liu, J. Sun, Y. Sun, Y. Xiang, Y. Yan, Z. Han, W. Bi, F. Yang, Q. Zhou, L. Wang, Y. Yu, *Chem. Eng. J.* **2020**, *394*, 124875.
[117] L. Zeng, M. Song, J. Gu, Z. Xu, B. Xue, Y. Li, Y. Cao, *Biomimetics* **2019**, *4*, 36.
[118] L. Wang, F. Deng, W. Wang, A. Li, C. Lu, H. Chen, G. Wu, K. Nan, L. Li, *ACS Appl. Mater. Interfaces* **2018**, *10*, 36721.
[119] M. Chen, J. Tian, Y. Liu, H. Cao, R. Li, J. Wang, J. Wu, Q. Zhang, *Chem. Eng. J.* **2019**, *373*, 413.
[120] Y. Li, L. Yang, Y. Zeng, Y. Wu, Y. Wei, L. Tao, *Chem. Mater.* **2019**, *31*, 5576.
[121] A. Pettignano, M. Häring, L. Bernardi, N. Tanchoux, F. Quignard, D. Díaz Díaz, *Mater. Chem. Front.* **2017**, *1*, 73.
[122] A. K. Sharma, Priya, B. S. Kaith, B. Shree, S. Saiyam, *React. Funct. Polym.* **2021**, *166*, 104977.
[123] Z. Wang, J. Zhou, H. Liang, S. Ye, J. Zou, H. Yang, *Prog. Org. Coat.* **2020**, *149*, 105943.
[124] H. Ye, C. Owh, S. Jiang, C. Z. Q. Ng, D. Wirawan, X. J. Loh, *Polymers* **2016**, *8*, 130.
[125] J. Chen, X. Ma, Q. Dong, D. Song, D. Hargrove, S. R. Vora, A. W. K. Ma, X. Lu, Y. Lei, *RSC Adv.* **2016**, *6*, 56183.
[126] S. Liu, D. Qi, Y. Chen, L. Teng, Y. Jia, L. Ren, *Biomater. Sci.* **2019**, *7*, 1286.
[127] M. Zheng, X. Wang, O. Yue, M. Hou, H. Zhang, S. Beyer, A. M. Blocki, Q. Wang, G. Gong, X. Liu, J. Guo, *Biomaterials* **2021**, *276*, 121026.
[128] Z.-X. Zhang, S. S. Liow, K. Xue, X. Zhang, Z. Li, X. J. Loh, *ACS Appl Polym Mater* **2019**, *1*, 1769.
[129] Y. Qin, J. Wang, C. Qiu, X. Xu, Z. Jin, *J. Agric. Food Chem.* **2019**, *67*, 3966.
[130] A. Mostafavi, H. Daemi, S. Rajabi, H. Baharvand, *Carbohydr. Polym.* **2021**, *257*, 117632.
[131] Z. Jing, A. Xu, Y. Q. Liang, Z. Zhang, C. Yu, P. Hong, Y. Li, *Polymers* **2019**, *11*, 952.
[132] X. Zhao, Y. Liang, Y. Huang, J. He, Y. Han, B. Guo, *Adv. Funct. Mater.* **2020**, *1910748*, 1.
[133] Y. Kobayashi, T. Hirase, Y. Takashima, A. Harada, H. Yamaguchi, *Polym. Chem.* **2019**, *10*, 4519.
[134] L. Zhao, Q. Zheng, Y. Liu, S. Wang, J. Wang, X. Liu, *Eur. Polym. J.* **2020**, *124*, 109474.
[135] L. Cai, R. E. Dewi, S. C. Heilshorn, *Adv. Funct. Mater.* **2015**, *25*, 1344.
[136] J. Qu, X. Zhao, Y. Liang, T. Zhang, P. X. Ma, B. Guo, *Biomaterials* **2018**, *183*, 185.
[137] J. He, M. Shi, Y. Liang, B. Guo, *Chem. Eng. J.* **2020**, 124888.
[138] S. Li, N. Chen, X. Li, Y. Li, Z. Xie, Z. Ma, J. Zhao, X. Hou, X. Yuan, *Adv. Funct. Mater.* **2020**, *2000130*, 1.
[139] Y. Yuan, S. Shen, D. Fan, *Biomaterials* **2021**, *276*, 120838.
[140] J. Savetsakulanont, J. Chalitangkoon, P. Monvisade, *Macromol. Mater. Eng.* **2021**, *306*, 2100287.
[141] C. Xu, W. Zhan, X. Tang, F. Mo, L. Fu, B. Lin, *Polym. Test.* **2018**, *66*, 155.
[142] X. Yang, M. Guo, Y. Wu, S. Xue, Y. Xia, R. Zhang, H. Wang, Q. Guo, *Mater. Res. Express* **2019**, *6*, 125340
[143] Q. Cheng, S. Ding, Y. Zheng, M. Wu, Y. Y. Peng, D. Diaz-Dussan, Z. Shi, Y. Liu, H. Zeng, Z. Cui, R. Narain, *Biomacromolecules* **2021**, *22*, 1685.
[144] J. Wen, Z. Jia, X. Zhang, M. Pan, J. Yuan, L. Zhu, *Polymers* **2020**, *12*, 239.
[145] D. qiang Li, S. ya Wang, Y. jie Meng, Z. wei Guo, M. mei Cheng, J. Li, *Carbohydr. Polym.* **2021**, *268*, 118244.
[146] C. Jiang, L. Zhang, Q. Yang, S. Huang, H. Shi, Q. Long, B. Qian, Z. Liu, Q. Guan, M. Liu, R. Yang, Q. Zhao, Z. You, X. Ye, *Nat. Commun.* **2021**, *12*, 4395.
[147] Y. Zhong, F. Seidi, C. Li, Z. Wan, Y. Jin, J. Song, H. Xiao, *Biomacromolecules* **2021**, *22*, 1654.
[148] Y. Luo, L. Fan, C. Liu, H. Wen, S. Wang, P. Guan, D. Chen, C. Ning, L. Zhou, G. Tan, *Bioact Mater* **2021**, *7*, 98.
[149] V. T. Tran, T. I. Mredha, J. Y. Na, J. Seon, J. Cui, I. Jeon, *Chem. Eng. J.* **2020**, *394*, 124941.
[150] R. R. Palem, K. Madhusudana Rao, T. J. Kang, *Carbohydr. Polym.* **2019**, *223*, 115074.
[151] N. J. Van Zee, R. Nicolaÿ, *Prog. Polym. Sci.* **2020**, *104*, 101233.
[152] S. Nevejans, N. Ballard, M. Fernández, B. Reck, S. J. García, J. M. Asua, *Polymer* **2019**, *179*, 121670.
[153] S. Bhattacharya, R. Hailstone, C. L. Lewis, *ACS Appl. Mater. Interfaces* **2020**, *12*, 46733.
[154] S. Liu, L. Li, *ACS Appl. Mater. Interfaces* **2017**, *9*, 26429.
[155] S. Jiang, S. C. Li, C. Huang, B. P. Chan, Y. Du, *Adv. Healthcare Mater.* **2018**, *7*, 1700894.
[156] G. S. Offeddu, J. C. Ashworth, R. E. Cameron, M. L. Oyen, *J. Mech. Behav. Biomed. Mater.* **2015**, *42*, 19.
[157] P. Zhao, H. Gu, H. Mi, C. Rao, J. Fu, L. Turng, *Front Mech Eng* **2018**, *13*, 107.
[158] E. J. Chung, M. Sugimoto, J. L. Koh, G. A. Ameer, *Tissue Eng., Part C* **2012**, *18*, 113.
[159] K. Katoh, T. Tanabe, K. Yamauchi, *Biomaterials* **2004**, *25*, 4255.
[160] M. P. Lutolf, J. A. Hubbell, *Nat. Biotechnol.* **2005**, *23*, 47.
[161] C. Heinemann, S. Heinemann, A. Lode, A. Bernhardt, H. Worch, T. Hanke, *Biomacromolecules* **2009**, *10*, 1305.

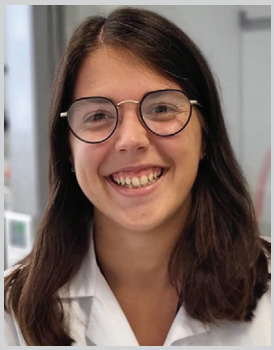

Mathilde Grosjean graduated as a chemical engineer from the National Graduate School of Chemistry of Montpellier in 2019. In 2020, she started a Ph.D. in the Department of Polymers for Health and Biomaterials of the Max Mousseron Biomolecules Institute (IBMM) in Montpellier, under the supervision of Prof. Benjamin Nottelet. Her Ph.D. project, funded by the French National Research Agency (ANR), aims to develop degradable biomaterials with actuation, bioadhesive, or self-healing properties for use in biomedical applications.

Louis Gangolphe graduated as Chemical Engineer from CPE Lyon in 2016. In 2020, he received his Ph.D. in Biomaterials at the University of Montpellier and the University of Grenoble Alpes. After working on the design of photocross-linked degradable elastomers for tissue reconstruction, he gained experience in biotechnology with the use of natural polymers and microfluidic technology to develop liver organoids for drug metabolism evaluation. He recently started a new adventure by joining Linxens as R&D Materials Engineer. His research interests focus on the use of functional polymer materials and their processing for biotechnology and medical devices sectors.

Benjamin Nottelet received his Ph.D. in Materials Chemistry from the University of Montpellier, France (2005). He was a post-doctoral fellow at ENSCM, France (2006) and in the Department of Pharmaceutics and Biopharmaceutics at the University of Geneva, Switzerland (2006–2008). In 2008, he joined the University of Montpellier and the Department of Artificial Biopolymers as an Associate Professor. He was appointed Full Professor in 2018 and is currently co-leader of the Department of Polymers for Health and Biomaterials of the IBMM. His research focuses on degradable and multifunctional polymers for biomedical applications in drug delivery, diagnostic, medical devices, and tissue engineering.